Redox Biology 42 (2021) 101959

Contents lists available at ScienceDirect

Redox Biology

journal homepage: www.elsevier.com/locate/redox

Peroxiredoxins wear many hats: Factors that fashion their peroxide sensing personalities

Jesalyn Bolduc [a,b,c], Katarina Koruza [a,b,c], Ting Luo [a,b,c], Julia Malo Pueyo [a,b,c], Trung Nghia Vo [a,b,c], Daria Ezeriņa [a,b,c], Joris Messens [a,b,c,*]

[a] VIB-VUB Center for Structural Biology, Vlaams Instituut voor Biotechnologie, B-1050, Brussels, Belgium
[b] Brussels Center for Redox Biology, Vrije Universiteit Brussel, B-1050, Brussels, Belgium
[c] Structural Biology Brussels, Vrije Universiteit Brussel, B-1050, Brussels, Belgium

ARTICLE INFO

Keywords:
Peroxiredoxin
Redox signaling
Post-translational modification (PTM)
Hydrogen peroxide (H_2O_2)
Protein-protein interactions (PPI)
Prx
Prdx

ABSTRACT

Peroxiredoxins (Prdxs) sense and assess peroxide levels, and signal through protein interactions. Understanding the role of the multiple structural and post-translational modification (PTM) layers that tunes the peroxiredoxin specificities is still a challenge. In this review, we give a tabulated overview on what is known about human and bacterial peroxiredoxins with a focus on structure, PTMs, and protein-protein interactions. Armed with numerous cellular and atomic level experimental techniques, we look at the future and ask ourselves what is still needed to give us a clearer view on the cellular operating power of Prdxs in both stress and non-stress conditions.

1. Introduction

1.1. The involvement of peroxiredoxins in cellular homeostasis

Peroxiredoxins (Prdxs) are a unique set of proteinsin several aspects: they have a high cellular abundance, are present in all known species, and in most cellular compartments [1–3]. They also display a variety of functions with the most well-known one being their role as peroxidase, but it is essential to point out that some Prdxs exhibit chaperone activity, while others exhibit phospholipase activity, although these functions are not a major focus of this review [4,5]. Prdxs are the most crucial proteins involved in maintenance of hydrogen peroxide (H_2O_2) levels by reduction, usually outcompeting other peroxidases in the cell like catalases and glutathione peroxidases (Gpxs) [7–9]. Thus, as Prdxs are the main regulators of H_2O_2 levels, and dysregulated H_2O_2 levels are linked to disease development [12], Prdxs are associated with pathogenesis and are therefore immensely important to understand.

Originally, Prdxs were called 'protector proteins' [13] and were known for helping cells survive oxidative stress conditions by reducing H_2O_2 [2], peroxynitrous acid, the protonated form of peroxynitrite (ONOOH) [14], and lipid peroxides [15]. This protection role was assigned to them for a long time as H_2O_2 was believed to only play a damaging and detrimental role [16]. However, in the past two decades it has become clear that at fine-tuned and controlled levels between 1 and 100 nM, H_2O_2 is required for the homeostatic signaling/functioning of the cell, simultaneously prompting the question of how Prdxs participate in cellular homeostasis [17–19]. Previously, Prdx involvement in signaling was only considered indirect. It was associated with their peroxidase function in controlling H_2O_2 levels (Fig. 1) and their inactivation by hyperoxidation, which would allow for H_2O_2 to accumulate and trigger cellular stress responses [1]. Recently, however, they have been recognized to also play a more direct and central role as cellular H_2O_2 sensors involved in signaling hubs for non-stress, homeostatic signaling [20,21]. They act as sensors by participating in "redox-relays" where oxidative equivalents are transferred from the Prdxs to the target protein by thiol-disulfide exchange [22,23] (Fig. 1). More explicitly, two possibilities exist for how this may occur. In one scenario, the thiol of the partner protein reacts with the sulfenic acid Prdx species, followed by thiol-disulfide exchange with a vicinal thiol in the partner, if available. In the other scenario, the thiol of the partner protein reacts with the disulfide within Prdx using a typical thiol-disulfide exchange mechanism. The transfer of oxidative equivalents to the target protein might affect the target's subcellular localization [24,25], structural conformation [26–28], and functionality [27,29,30]. Notably, Prdxs appear to be promiscuous, connecting with many different target proteins within structural complexes located in cellular microdomains [31,32]. This

* Corresponding author. VIB-VUB Center for Structural Biology, Vlaams Instituut voor Biotechnologie, B-1050, Brussels, Belgium.
E-mail address: joris.messens@vub.be (J. Messens).

https://doi.org/10.1016/j.redox.2021.101959
Received 29 November 2020; Received in revised form 7 March 2021; Accepted 25 March 2021
Available online 20 April 2021

connects Prdxs to most key signaling networks responsible for cellular responses to both stress and non-stress messages, implicating them in overall cellular metabolism, fitness, and survival. However, only a handful of interactions (STAT3, ASK1, TIMELESS) have been explored in mechanistic detail [20,21,31,33,34] and even still, many questions remain. To further complicate matters, the Prdxs are also subject to post-translational modifications (PTMs), which regulate/control/organize their scavenging, signaling, and regulating functions [4,35–47].

Thus, it seems that as much as we have learned about Prdxs, they continue to reveal additional, intriguing facets of themselves, and there is much unexplored territory around this fascinating family of enzymes. In this review, we begin with a tabulated overview of what is known about human and bacterial Prdxs in terms of structure and PTMs. We decided not to touch upon yeast Prdxs as they often display characteristics of both human and bacterial Prdxs, making them difficult to categorize. We summarize the methods and techniques that are being used to investigate Prdxs and the protein-protein interactions (PPI) they are involved in, and we conclude with a perspectives section highlighting the anticipated and required progress for this field of study in the next quinquennial.

1.2. Key mechanistic features of peroxiredoxins

In the social theory of intersectionality [48], an individual's identity is influenced by many intersectional identities, meaning the identities are intertwined and interdependent, but not necessarily overlapping: race, gender, class, location, age, etc. It is similar for Prdxs in determining their functional identity. The functional identity (i.e. peroxidase, redox-relay participant, or other function) of a Prdx is determined by many "intersectional" factors. There are more factors than what will be covered in this review, but here the focus will be given to subgroup category, oligomeric state, protein motifs, redox state, and PTMs. Because these factors are intersectional, they are described together as it is difficult to explain one without referencing the others.

There are six different subgroups of Prdxs: Prdx1/AhpC, Prdx5, Prdx6, Tpx, BCP/PrdxQ, and AhpE. Typical, 2-Cys Prdxs (Prdx1 subgroup; mammalian Prdx1-4) and the 1-Cys Prdx (mammalian Prdx6) exist as obligate homodimers. Depending on the redox state and/or certain PTMs present (i.e. phosphorylation, acetylation), the typical, 2-Cys Prdxs can oligomerize further into a decameric (or pentamer of dimers), or dodecameric (hexamer of dimers) toroid structure (Fig. 2) [49,50]. The reduced decamer is the most efficient peroxidase because of allosteric "buttressing" that makes a more fully-folded, stable active site. These toroid structures, depending on their redox state or additional PTMs present, can stack with one another to form high molecular weight (HMW) oligomers that look like "filaments", which are associated with cell-cycling checkpoints [51] and in some cases, chaperone activity [36,52]. The atypical, 2-Cys Prdxs (mammalian Prdx5) were originally described as monomeric proteins [53]. However, through an alternative interface observed in all Prdx5 structures, dimerization occurs, even independently of the redox state [3].

All the Prdxs progress through the typical 2-Cys Prdx catalytic cycle represented in Fig. 1 essentially the same way. This cycle is covered extensively in detail elsewhere [54–56]. In brief, during the catalytic cycle, the reduced peroxidatic cysteine (Cys_P) is oxidized to a Cys sulfenic acid (Cys_P–SOH), which is resolved by reaction with the resolving cysteine (Cys_R) to form a disulfide (Cys_P-S-S-Cys_R). Despite all Prdxs going through this same cycle, the point of difference comes from whether the Cys_R, depending on the functional identity of the Prdx at the time, comes from the adjacent monomer, the same monomer, or a separate nucleophile like glutathione or a redox-relay binding partner (Fig. 1). At least in the case of typical, 2-Cys Prdxs, we know that disulfide formation between Cys_P and Cys_R of the adjacent monomer

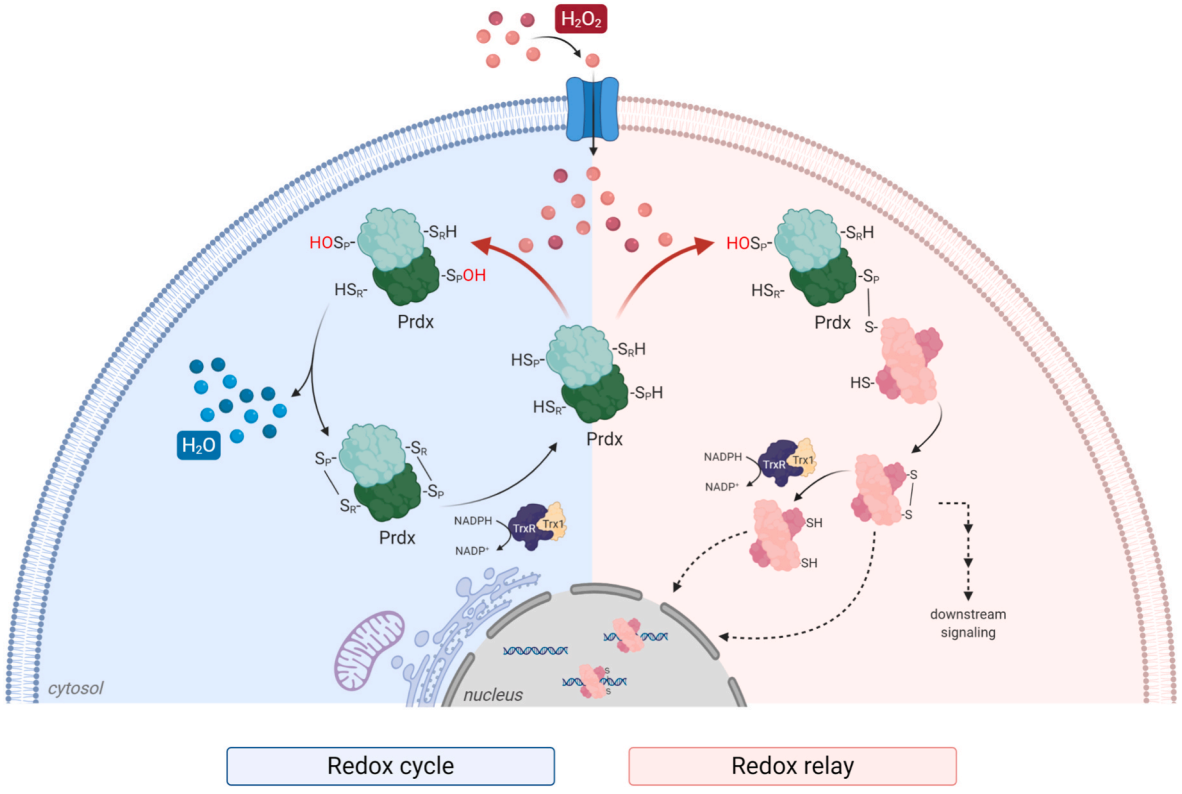

Fig. 1. Mechanism of the redox cycle and the redox-relay of typical 2-Cys Prdxs (shown family members are the cytosolic human Prdx1 and Prdx2). *Prdx scavenges H_2O_2 through the formation of a sulfenic acid (Cys-SOH) on the peroxidatic cysteine (Cys_P) with the subsequent formation of a disulfide bond between Cys_P and the resolving cysteine (Cys_R)* [10]. *Prdx is recycled via the thioredoxin pathway (Trx-TrxR-NADPH)* [11]. *Via a redox-relay, oxidative equivalents can be transferred to a binding partner in a process that, depending on the partner, may involve an additional scaffold protein.*

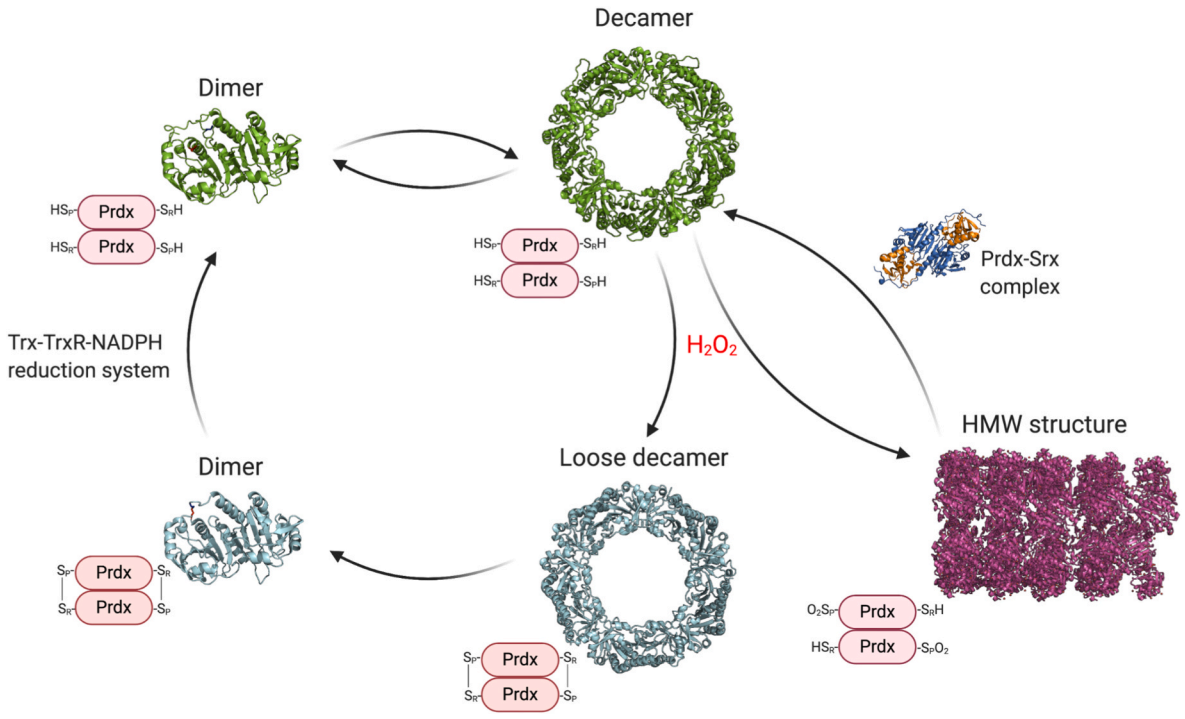

Fig. 2. Oligomeric states of Prdxs. *There is dynamic equilibrium between dimer and decamer when Prdx is reduced, with the reduced (SH) decamer being the most efficient. Oxidation loosens the decamers causing them to dissociate back into dimers. The structures depicted are WT Salmonella typhimurium Prdx1/AhpC (reduced form (green): 4MA9; oxidized form (light blue): 1EYP). The decamers can stack also to form HMW oligomers, and this is usually linked to overoxidation, like what is shown in purple (human Prdx3:* 5JCG*). Overoxidized Prdxs are repaired by sulfiredoxin (Srx) in an ATP-dependent mechanism, shown with the Prdx-Srx complex structure (dark blue, human Prdx1: 2RII).* (For interpretation of the references to colour in this figure legend, the reader is referred to the Web version of this article.)

requires quite a bit of local structural rearrangement, which affects the overall oligomeric state. The helix containing the Cys_P must unwind and flips outwards to meet the Cys_R, which is in the C-terminal region. This C-terminal region is a semi-flexible region and is often difficult to capture in X-ray structures until the disulfide forms, as this "locks" the terminal region into an ordered state (Fig. 3, panel b and c). These structural rearrangements destabilize the decamer, making it "loose", and ultimately causing it to dissociate back into dimeric subunits (Fig. 2) [6,50]. The Cys_P-S-S-Cys_R is then reduced by the NADPH-dependent thioredoxin-thioredoxin reductase system.

The difference across the subgroups is that the atypical, 2-Cys types contain two Cys residues in the monomeric subunit of the obligate homodimer, while the 1-Cys types get the resolving electron donor from another source, like glutathione [3,57,58]. Also, of note, 1-Cys Prdxs are incredibly robust against inactivation via overoxidation (-SO_2H or –SO_3H formation) [57], also known as hyperoxidation. Hyperoxidized Prdxs are repaired by the ATP-dependent sulfiredoxin enzyme, but human Prdx6, a 1-Cys Prdx, does not interact with sulfiredoxin [57].

In terms of resistance against hyperoxidation, there are pronounced differences between bacterial and human Prdxs. Mammalian Prdxs1-4, despite being in the same subgroup as the bacterial AhpC, are significantly more prone to being overoxidized than AhpC, and this was

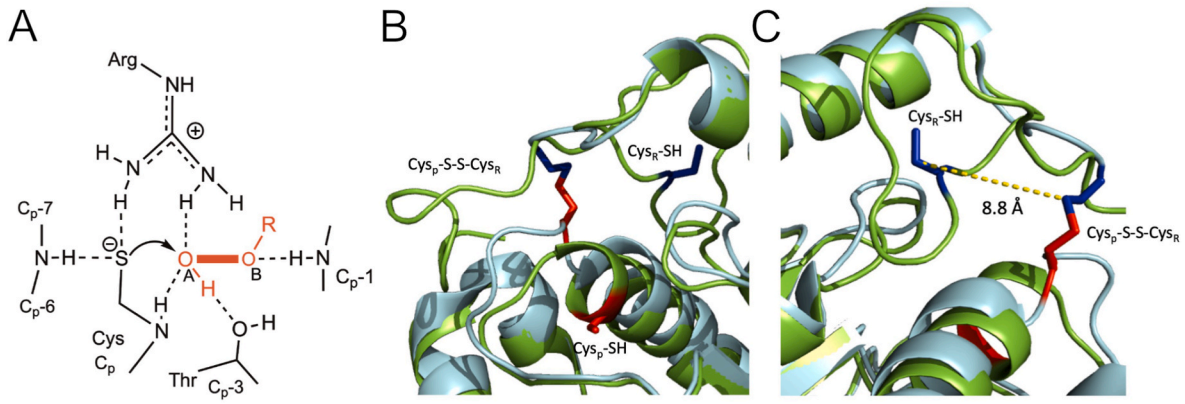

Fig. 3. Active site organization of peroxiredoxins. ***A.*** *The low pKa of the peroxidatic cysteine (Cys_P) and the conserved hydrogen bonding network that stabilizes the transition state determine the high second order rate constant of H_2O_2 sensing. Adapted from Hall* et al. [6]. ***B.*** *The formation of the intersubunit disulfide bond (Cys_P-S-S-Cys_R) in the presence of H_2O_2 requires the structural rearrangement of the active site from a fully folded (green) to a locally unfolded (light blue) loop for the Cys_R-S to access the oxidized Cys_P-S.* ***C.*** *The distance between the resolving Cys in the reduced (Cys_R-SH) and oxidized (Cys_R-S-) peroxiredoxin is shown. The structures depicted in b) and c) are WT Salmonella typhimurium Prdx1/AhpC (reduced form (green): 4MA9; oxidized form (blue): 1EYP).* (For interpretation of the references to colour in this figure legend, the reader is referred to the Web version of this article.)

determined to be because eukaryotic Prdxs contain the GGLG and YF motifs that render them "sensitive" [2,3]. It is believed that the GGLG and YF motifs confer sensitivity to hyperoxidation by slowing down the structural rearrangements of the C-terminus necessary forCys_P-S-S-Cys_R formation. Later, two additional motifs, Motifs A and B, were discovered that confer resistance to overoxidation across the eukaryotic and prokaryotic Prdx distinction [59]. This helped explain the stratification of overoxidation sensitivity observed across Prdx subgroups, but it blurred the lines of known Prdx categorization.

Indeed, it is difficult to neatly phylogenetically sort these enzymes [60]. Despite the difficulty with categorization, the theme of redox sensing is conserved in Prdxs along with the conservation of the redox sensitive, active site Cys, the Cys_P. The Cys_P has a *pKa* value in the range of 5–6.3 [61–63]. However, whereas most deprotonated thiols react with H_2O_2 with a rate constant of ~1–10 $M^{-1}s^{-1}$, the Cys_P residue of Prdxs reacts with H_2O_2 with rate constants of 10^5–10^7 $M^{-1}s^{-1}$ [8,64,65]. The low *pKa* alone appears to be insufficient to account for the high reactivity of Prdxs with H_2O_2. The unusually high reaction rate is attributed to the fact that Prdxs activate not only the thiolate of Cys_P but also one of the oxygens of H_2O_2 via a conserved hydrogen bonding (H-bonding) network, which renders one of the oxygens more susceptible to nucleophilic attack by the thiol sulfur [6] (Fig. 3, panel a). For some subgroups, the active site H-bonding network can display notable differences. For example, the Cys–SOH species of the 1-Cys Prdx6 has a slightly shifted H-bonding network (compared to the typical 2-Cys Prdx1/AhpC subclass) that includes a histidine that is unique for this subclass. However, this does not affect the rate constant of Prdx6 which is similar to that of 2-Cys Prdxs [66].

In summary, Prdxs can be regarded as the peroxide sensors of the cell, assessing peroxide levels and controlling the subsequent action needed to be taken by the cell to optimize metabolism, maintain cellular integrity and fitness of the cell and to survive environmental changes [67]. However, to effectively do this, Prdxs must play many functional roles, which are controlled by many different parameters. We review some of them here for bacteria (excluding yeasts and archaea for the sake of readability) and humans. To reiterate, it is absolutely critical to learn more about Prdxs as they play such a key role in cellular (patho) physiology. Although a lot of information on available structures, PTMs, and interaction partners, studied with numerous different methods, is available, many more questions remain to be answered.

2. A structural summary of peroxiredoxins

As of November 2020, the search term for macromolecular identifier "peroxiredoxin" in the RCSB protein databank yields 113 entries for structures under the "*Homo sapiens*" category and 138 structures under the "Bacteria" category, with 135 being X-ray diffraction structures and the other 3 being NMR structures. All but one of the human structures were solved using X-ray diffraction, and one was solved by NMR. From the 113 human structures, 35 are included in Tables 1 and 2. The rest of the results come from human proteins functionally similar or

Table 1
Human Peroxiredoxin structures in the reduced form.

Name	PDB Code	Oligomeric state	Reference
Prdx4	3TKP	decamer	[69]
Prdx4	3TKS	decamer	[69]
Prdx4 C51S[a]	3TJF	decamer	[70]
Prdx4 T118E	3TKR	decamer	[69]
Prdx4 C245A	3TJK	decamer	[70]
Prdx5	1HD2	dimer[b]	[53]
Prdx5	1H4O	dimer	[53]
Prdx6	5B6M	dimer	[71]

[a] = despite the C_P mutation, the active site conformation looks like wildtype SH.
[b] = symmetry dimer with one molecule in the asymmetric unit.

Table 2
Additional human Prdx structures.

Name	PDB Code	Redox State	Description	Oligomeric State	Reference
Prdx1	2RII	SS	C_P in disulfide with sulfiredoxin	hetero tetramer	[72]
Prdx1 C52D/ A86E	3HY2	SS-like	In complex with sulfiredoxin (C99A) and ATP:Mg^{2+}; active site similar to SS despite C_P mutation	hetero tetramer	[73]
Prdx1 C83S	4XCS	SS	Oxidation/ disulfide formation of the active site C_P with the C_R	dimer	[74]
Prdx2	1QMV	SO_2H	S-sulfinylation of the active site C_P	decamer	[75]
Prdx2	5IJT	SS	Oxidation/ disulfide formation of the active site active site C_P with the C_R	decamer	[59]
Prdx3 S78C	5UCX	SH	3 ring stack (HMW) form	dodecamer	[76]
Prdx3	5JCG	SH	3 ring stack (HMW) form	36-mer (3 stacked dodecamers)	[76]
Prdx4 C51A	3TJG	SS-like	Active site resembles SS despite C_P mutation	decamer	[70]
Prdx4 C245A	3TJJ	SOH	S-sulfenylation of the active site C_P	decamer	[70]
Prdx4	3TKQ	Mixed SOH and SO_2H	S-sulfenylation/ sulfinylation of the active site C_P	decamer	[69]
Prdx4	3TJB	SS	Oxidation/ disulfide formation of the active site C_P with the C_R	decamer	[70]
Prdx4 C-term	3W8J	–	C-term only of Prdx4 in complex with P5 a0	monomer	[77]
Prdx4 C-term	3WGX	–	C-term only in complex with ERp46 Trx2	monomer	[78]
Prdx4 T118E/ C14S/ C87S	5HQP	SS	C_R in disulfide with Cys29 of ERp44	hetero tetramer	[79]
Prdx4	4RQX	SS	Disulfide between C124 and BNP7787 (MESNA)	decamer	[80]
Prdx5 C72S	2VL9	SS (some SH)	Oxidation/ disulfide formation of the active site C_P with the C_R	dimer	[81]
Prdx5 C72S	2VL3	SS (some SH)	Oxidation/ disulfide formation of the active site C_P with the C_R	dimer	[81]
Prdx5 C72S	2VL2		Oxidation/ disulfide	dimer	[81]

(*continued on next page*)

Table 2 (*continued*)

Name	PDB Code	Redox State	Description	Oligomeric State	Reference
		SS (some SH)	formation of the active site C_P with the C_R		
Prdx5	3MNG		with oxidized DTT bound in active site	dimer	[82]
Prdx5	4K7I	–	with an analogous fragment based on DTT (3MNG structure)	dimer	[83]
Prdx5	4K7N	–	with an analogous fragment based on DTT (3MNG structure)	dimer	[83]
Prdx5	4K7O	–	with an analogous fragment based on DTT (3MNG structure)	dimer	[83]
Prdx5	4MMM	–	withan analogous fragment based on DTT (3MNG structure)	dimer	[83]
Prdx5	1OC3	SS	Oxidation/ disulfide formation of the active site C_P with the C_R	dimer	[84]
Prdx5 C47S	1URM	–	Benzoate ion in active site	dimer	[85]
Prdx6	5B6N	SOH	S-sulfenylation of the active site C_P	dimer	[71]
Prdx6 C91S	1PRX	SOH	S-sulfenylation of the active site C_P	dimer	[86]

functionally related to Prdxs, for instance, thioredoxin and glutaredoxin. Among the human Prdx structures, there are 8 reduced structures, and generally speaking, Prdx4 and 5 have the most information, with 13 and 12 structures, respectively. The human Prdxs that have the least amount of structural information are Prdx2 and 3, with two structures solved for each. There are 12 structures where a Prdx is in complex with a ligand, either another protein (5 PDB entries) or a small molecule (7 PDB entries). However, there is not a single human Prdx structure solved with H_2O_2 nor any other oxidizing substrate bound in the active site.

For bacteria, 72 of these bacterial structures are included in Tables 3 and 4 and the remaining structures are of proteins related to bacterial Prdx function, such as AhpD and AhpF. Also, some other structures were omitted from the tables because they were submitted to the PDB, but never published, therefore much of the information the structure provides is not yet shared with the scientific community. Out of the 72 structures in Tables 3 and 4, 32 of them are Prdxs in versions of the reduced form. The bacterial Prdx with the most structural information is AhpC, with 15 *Salmonella typhimurium* structures and 11 additional AhpC structures from a menagerie of other organisms. There are some structures available for bacterial Prdxs where peroxides are in the active site (*V. vulnificus* from Table 4, PDB code 5K2J; archaeon *A. pernix K1*, thus excluded from this review in detail, but PDB code 3A2V- H_2O_2 actually bound in active site), but because of the expanse of bacterial species, the structures that still need to be solved are immense and difficult to actually tally, making it clear that much information about bacterial Prdxs is still needed [68].

As evident in Tables 1–4 and mentioned in the introduction, Prdxs exist in several different oligomeric states: monomer, dimer, decamer, dodecamer, and HMW oligomers. The flux between these different states often depends on the redox state of the Prdx as well as any PTMs that may be present, like the ones mentioned in Tables 5 and 6. However, no structure of a Prdx with a PTM has been solved.

Table 3
Bacterial Prdx structures in reduced and mixed form

Organism and Name	PDB Code	Redox State	Oligomeric State	Reference
Escherichia coli/ Homo sapiens chimera				
AhpC1-186-YFSKHN	5B8B	SH	decamer	[87]
Salmonella typhimurium				
AhpC T43S	4XRA	SH (FF)	decamer	[54]
AhpC T43A	4XTS	SH (LU)	decamer	[54]
AhpC T43V	4XS1	SH (LU)	decamer	[54]
AhpC E49Q	5UKA	SH (alternative FF arrangement)	pentamer	[54]
AhpC C46S	1N8J	SH-like (FF)	decamer	[2]
AhpC	4MA9	SH	decamer	[55]
AhpC C165A	4MAB	SH, destabilized C terminus	decamer	[55]
Enterococcus faecalis				
AhpC	5Y63	SH (FF & LU)	decamer	[88]
Haemophilus influenza				
Prdx5 hybrid w/Grx	1NM3	SH	tetramer	[89]
Mycobacterium tuberculosis				
AhpE	1XXU	SH with bromide ion	dimer	[90]
AhpE	4X0X	SH**	dimer	[91]
AhpE F37H	5C04	SH**	dimer	[92]
AhpE R116A	4XIH	SH**	dimer	[92]
Tpx C60S	1Y25	SH-like (FF)	dimer	[93]
Akkermansia muciniphila				
Prdx	6KHX	SH	decamer	[94]
				[95]
Xanthomonas campestris				
PrdxQ	5IIZ	SH	monomer	[56]
PrdxQ	5IM9	SH (90%)	monomer	[56]
PrdxQ	5IMC	SH (50%)*	monomer	[56]
PrdxQ	5IMF	SH (50%)*	monomer	[56]
PrdxQ C48S	5IO2	SH-like	monomer	[56]
PrdxQ	5IMA	SH (55%)*	monomer	[56]
PrdxQ	5IMD	SH (60%)*	monomer	[56]
PrdxQ	5IMV	SH (55%)*	monomer	[56]
PrdxQ	5IMZ	SH (55%)*	monomer	[56]
PrdxQ C84S	5IPH	SH-like (FF)	monomer	[56]
BCP	3GKM	SH	monomer	[96]
Escherichia coli				
Tpx C61S	3HVV	SH-like (FF)	dimer	[97]
Tpx C61S	4AF2	SH-like (FF)	dimer	[98]
Yersina pseudotuberculosis				
Tpx	2YJH	SH-like (FF)	dimer	[99]

*=mixed population containing oxidized species like SO, SO_2H and/or SO_3H.
**=different hydrogen bond network arrangement for active site in comparison to canonical active site hydrogen bond network.
FF=fully-folded active site.
LU=locally-unfolded active site.
SH-like=a C_P mutant that still maintains the active site conformation similar to SH.
SO_2H-like=a C_P mutant that still maintains the active site conformation similar to SO_2H.

Table 4
Other bacterial Prdx structures

Organism Name	PDB Code	Redox State	Description	Oligomeric state	Reference
Escherichia coli/Homo sapiens chimera					
AhpC1-186-YFSKHN	5B8A	SS	Oxidation/disulfide formation of the active site C_P with the C_R	decamer	[87]
Escherichia coli					
AhpC	4O5R	SS	Oxidation/disulfide formation between active site C_P and the C_R	decamer	[100]
AhpC trunc 1-172	4QL7	SS	Oxidation/disulfide formation between active site C_P and the C_R	decamer	[101]
AhpC trunc 1-182	4QL9	SS	Oxidation/disulfide formation between active site C_P and the C_R	decamer	[101]
AhpC1-186-YFSKHN	5B8A	SS	Oxidation/disulfide formation between active site C_P and the C_R		
Tpx	3HVS	SS	Oxidation/disulfide formation between active site C_P and the C_R	dimer	[97]
Tpx	3I43	SS (alt conf)	Oxidation/disulfide formation between active site C_P and the C_R but with an alternative conformation	dimer	[97]
Tpx	1QXH	SS	Oxidation/disulfide formation between active site C_P and the C_R	dimer	[102]
Tpx C82,95S	3HVX	SS (Cys_p-Cys_p)	Oxidation/disulfide formation between active site C_P and the C_P of another Tpx	dimer	[97]
Aquifex aeolicus VF5					
AhpC2	5OVQ	SO_3H	S-sulfonylation of the active site C_P	dodecamer	[103]
Salmonella typhimurium					
AhpC	1YEP	SS	Oxidation/disulfide formation between active site C_P and the C_R	decamer	[49]
AhpC T77I	1YF0	SS	Oxidation/disulfide formation between active site C_P and the C_R	decamer	[49]
AhpC T77V	1YF1	SS	Oxidation/disulfide formation between active site C_P and the C_R	decamer	[49]
AhpC T77D	1YEX	SS	Oxidation/disulfide formation between active site C_P and the C_R	decamer	[49]
AhpC C165S	4XS4	SH/SS (FF/LU)	Oxidation/disulfide formation between active site C_P crystallized with DTT	decamer	[54]
AhpC W81F	4XS6	SS (LU)	Oxidation/disulfide formation of between active site C_P crystallized with DTT	decamer	[54]
AhpC W169F	4XRD	SH/SS (FF/LU)	Oxidation/disulfide formation of between active site C_P crystallized with DTT	decamer	[54]
AhpC C165S	3EMP	S-acetanilide on C46		decamer	[61]
Amphibacillus xylanus					
AhpC	1WE0	SS	Oxidation/disulfide formation between active site C_P and the C_R	decamer	[104]
Mycobacterium tuberculosis					
AhpC	2BMX	SS	Oxidation/disulfide formation between active site C_P and the C_R	dodecamer	[105]
AhpE	1XVW	SS	Oxidation/disulfide formation between active site C_P and the C_R	octamer	[90]
AhpE	5ID2	SOH/SH	S-sulfenylation of active site cysteine	dimer	[106]
AhpE	4X1U	SOH with a different hydrogen bond network	S-sulfenylation of active site C_P	monomer	[91]
Tpx	1XVQ	SOH	S-sulfenylation of the active site C_P	monomer	[107]
Helicobacter pylori					
AhpC	1ZOF	SS	Oxidation/disulfide formation between active site C_P and the C_R	decamer	[108]
Vibrio vulnificus					
Prdx3	5K2I	SS	Oxidation/disulfide formation between active site C_P and the C_R	dimer	[95]
C73S					
Prdx3	5K2J	–	H_2O_2 present in active site but not bound due to mutation	dimer	[95]
C48D/C73S					
Prdx3 C48D/C73S	5K1G	SO_2H-like	Active site similar to S-sulfinylation of the active site C_P	dimer	[95]
Xanthomonas campestris					
PrdxQ	5IO0	SO_2H	S-sulfinylation of the active site C_P	monomer	[56]
PrdxQ	5IOW	SO_2H	S-sulfinylation of the active site C_P by cumene peroxide	monomer	[56]
PrdxQ	5IPG	SO_2H	S-sulfinylation of the active site C_P by *t*-butyl peroxide	monomer	[56]
PrdxQ	5IOX	SS	Oxidation/disulfide formation between active site C_P and the C_R	monomer	[56]
PrdxQ	5IPH	SO_2H	S-sulfinylation of the active site cysteines	monomer	[56]
C84S					
PrdxQ	5INY	SO_2H	S-sulfinylation of the active site cysteines	monomer	[56]
BCP	3GKN	SS	Oxidation/disulfide formation between active site C_P and the C_R	dimer	[96]
BCP	3GKK	SS	Oxidation/disulfide formation between active site C_P and the C_R	dimer	[96]
Yersinia pseudotuberculosis					
Tpx	3ZRD	SS	Oxidation/disulfide formation between active site C_P and the C_R	dimer	[99]
Tpx	2XPE	SS	Oxidation/disulfide formation between active site C_P and the C_R	dimer	[99]
Thermotoga maritima					
TmNtrPrdx C40S	4EO3	–	A unique hybrid protein containing an N-terminal 1-Cys PrxBCP domain fused to a flavin mononucleotide-containing nitroreductase (Ntr) domain	dimer	[109]

3. Peroxiredoxin modulation through various post-translational modifications

Human Prdxs are regulated by a variety of PTMs, including, but not limited to: acetylation, ubiquitination, glutathionylation, different types of oxidation (SOH, SS, SO_2, SO_3), S-nitrosylation, and phosphorylation [4]. There is also observation of tyrosine nitration in peroxiredoxins [110,111]. There have been 26 modified residues identified by low-throughput methods amongst the 6 different human isoforms: 10 for Prdx1, 5 for Prdx2, 2 for Prdx3, and 5 for Prdx6 (Table 5). For high-throughput methods, the residues have been identified through mass spectrometry (MS)-based proteomics and are summarized in Table 10. Notably, however, limited residues have been further verified *in vivo* through additional investigative methods. For example, phosphorylation of human Prdx1 has been detected on Thr18, Ser32, Thr90, Thr156, Thr183, Tyr194 by proteomics studies, but only Ser32, Thr90, Thr183, Tyr194 have been confirmed by immunoblot probing cell lysates. In fact, commercial antibodies have now been developed that recognize Thr90 and Tyr194. The other putative phosphorylation sites remain to be substantiated. PTM detection is discussed at further length

Table 5
Human Prdx PTMs identified by low-throughput methods.

Name	Residue	PTM	Functional consequence	Reference
Prdx1	Cys^{52}, Cys^{83}, Cys^{173}	GSH	Loss of chaperone activity; shift from decamer to dimer; protection against hyperoxidation	[114]
Prdx2	Cys^{51}, Cys^{172}	GSH	Protection against hyperoxidation	[115]
Prdx6	Cys^{47}	GSH	Regeneration of the reduced Cys_P	[58]
Prdx1	Thr^{90}, Thr^{183}, Ser^{32}, Tyr^{194}	P	Inhibits peroxidase activity; increases decamer formation and chaperone activity; except Ser32 which enhanced peroxidase activity	[37–39]
Prdx2	Ser^{76}*, Thr^{89}	P	Thr89 inhibits peroxidase activity and enhanced decamer formation and chaperone activity; * indicates that Ser76 was only identified through a mutational study	[43,116]
Prdx6	Thr^{177}	P	Increases phospholipase A_2 activity	[46]
Prdx1	Lys^{197}, Lys^{27}	Ac	Lys197 acetylation increases peroxidase activity, and hyperoxidation resistance; Lys27 acetylation enhances chaperone activity	[41,42]
Prdx2	Lys^{196}	Ac	Acetylation of Prdx increases peroxidase activity and hyperoxidation resistance	[42]
Prdx3	Lys^{253}	Ac	Inhibits peroxidase activity	[45]
Prdx6	Lys^{unk}	Ac	Unknown	[117]
Prdx1	Lys^{unk}	Ub	Causes degradation	[44,118]
Prdx3	Lys^{unk}	Ub	Causes degradation	[119]
Prdx6	Lys^{122}, Lys^{142}	Sm	Increased GSH-peroxidase and $aiPLA_2$ activity	[120]
Prdx1	Cys^{51}	SNO	Inhibits peroxidase activity; enhances chaperone activity	[40]
Prdx2	Cys^{51}, Cys^{172}	SNO	Inhibits peroxidase activity	[47]
Prdx5	Cys^{48}	SCoA	Inhibits peroxidase activity	[121]
Prdx2	Cys^{51}	SSH SSOH SSO_2H	Protection against hyperoxidation	[112]

GSH= Glutathionylation; P= Phosphorylation; Ac=Acetylation; Ub=Ubiquitination; Sm=SUMOylation SNO=S-nitrosylation; SCoA= S-coAlation; SSH – persulfidation; SSOH – perthiosulfenic acid; SSO_2H – perthiosulfinic acid.

in the methods section.

In general, the validated PTMs for bacterial Prdxs are much less diverse than those known for human ones and mostly include redox modifications of the catalytic Cys (Table 6 and see also references in Table 4 for the oxidative PTMs), even though high-throughput studies have additionally yielded phosphorylation and acetylation sites on some, as indicated in Table 11. Despite the small number of PTMs reported, PTMs of Prdxs belonging to different classes (i.e., both 1-Cys and 2-Cys) and organisms have been identified. Specifically, those redox PTMs are the formation of sulfenic acid (SOH) upon the reaction with H_2O_2, peroxynitrite, or other peroxides, products of overoxidation to sulfinic acid (SO_2H) (5 examples on 4 different Prdxs from 3 organisms), as well as the products of the reaction of the sulfenic acid with a low molecular weight thiol such as glutathione or mycothiol, a first step to the regeneration of the catalytic thiol (3 examples on 3 Prdxs from 2 organisms).

An interesting modification, that has also been reported for human Prdx2 [112] is the persulfidation of the catalytic Cys of AhpE that occurs via the reaction of the sulfenic acid with H_2S. The resulting persulfide can then be reduced back to the thiol by reacting with another molecule of H_2S, or another thiol. As this reaction occurs at a sufficient rate for the catalytic cycle to restart, it can be considered an alternative reduction mechanism to the MSH/Mrx-1/Mtr system. Moreover, persulfidation may be a way for modulating the function of AhpE, as persulfidation lowers the reactivity of AhpE to peroxides, yet enables it to act as a transpersulfidase [113]. This intriguing additional layer of PTMs being

Table 6
Bacterial Prdx PTMs identified by low-throughput methods.

Name	Residue	PTM	Description	Reference
Mycobacterium tuberculosis				
AhpE	Cys^{45}	SOH/ SO_2H	Product of oxidation upon the reaction with peroxynitrite (-SOH) and H_2O_2 (-SOH and $-SO_2H$)	[63]
AhpE	Cys^{45}	MSH	Reduction of the sulfenic acid formed on the catalytic Cys by Mrx-1/Mtr, which proceeds via a monothiol mechanism; protection from overoxidation	[122]
AhpE	Cys^{45}	SSH	H_2S reacts with the sulfenic acid formed on the catalytic Cys, forming a persulfide, which can then be reduced back to a thiol by another molecule of H_2S or another thiol. As this reaction occurs at a rate sufficient for the catalytic cycle to restart, it constitutes an alternative mechanism of reduction to the MSH/Mrx-1/Mtr system. Persulfidation of AhpE also enables it to be involved in transpersulfidation.	[113]
Corynebacterium glutamicum				
Mpx	Cys^{36}	SOH	Product of reaction with H_2O_2	[123]
Mpx	Cys^{36}	MSH	Reduction of the sulfenic acid formed on the catalytic Cys by Mrx-1/Mtr, which proceeds via a monothiol mechanism, though it can also be reduced by Trx via a dithiol mechanism; protection from overoxidation	[123]
Tpx	Cys^{60} Cys^{94} Cys^{81}	MSH	Reduction of the sulfenic acid formed on the catalytic Cys (Cys^{60}) by Mrx-1/Mtr, which proceeds via a monothiol mechanism; protection from overoxidation	[124]
Escherichia coli				
Tpx	Cys^{61}	SOH/ SO_2H	Oxidation product upon the reaction with H_2O_2 and cumene hydroperoxide	[125]
BCP	Cys^{45}	SOH	Oxidation product with H_2O_2 and other peroxides	[126]
Model cyanobacterium *Synechocystis* sp. PCC6803				
Sll1621 (PrdxII)		GSH	Bioindication purposes (proposed effect of PTM)	[127]

SOH – formation of a sulfenic acid; SO_2H – formation of a sulfinic acid; MSH = S-mycothiolation; SSH = persulfidation; GSH = S-glutathionylation.

able to modulate the function of Prdxs warrants further investigation of PTMs of bacterial Prdxs.

4. Additional methods useful for investigating peroxiredoxins

50 years ago, transmission electron microscopy (TEM) yielded the first images of an erythrocyte protein (Prdx2) with an apparent tenfold symmetry oligomerization [128]. Since then, the combination of the continuously expanding repertoire of methods used to investigate Prdx has allowed the visualization of the Prdx structure on multiple scales, from individual oligomeric states to HMW assemblies of stacked decamers, and even surveilling different forms in living cells in real time [116]. Table 7 summarizes the experimental techniques that have been used for investigating Prdxs.

As the redox-relay function of Prdxs has come more into focus, PPI techniques have been used to identify redox-relay partners of Prdxs. For identifying Prdx interactomes, there are two main methods: immunoprecipitation (or affinity pulldown; IP) in tandem with MS or the yeast two hybrid system followed by co-immunoprecipitation. However, several other methods can also be utilized, including native PAGE separation, 2-dimensional gel electrophoresis, Bio-ID, iPOND (isolation of protein on nascent DNA), and kinetic trapping coupled with a variety of MS-based techniques such as LC-MS/MS, NanoLC-MS/MS, HPLC-MS, and MudPIT (MS-based multidimensional protein identification technology). The techniques that have been successfully utilized before are summarized in Table 8, along with the Prdx interactors they helped to identify.

For verifying specific interactors beyond initial MS identification, co-immunoprecipitation (or co-affinity pulldown) is the most predominant approach for *in vivo* validation. Other alternative approaches are proximity-based immunofluorescence (PLA, etc.), yeast two-hybrid and co-localization immunofluorescence for *in vivo* confirmation. While all the previous methods are employed in cells or cell lysates, there are some examples of *in vitro* verification techniques including: maintaining protein-complex in chromatography, the pre-co-incubation of two interactors followed by SDS-PAGE and MS analysis or even confirmation of protein interaction by X-ray crystallography co-crystallization. However, sometimes protein complexes may be difficult to maintain *in vitro* for numerous reasons, such as missing facilitator proteins, dissociation of the weak interactions, etc. The techniques used for PPI validation for Prdxs are tabulated in Table 9 along with the interaction partner the technique helped confirm.

In addition, there are tools available for PTM identification and verification. Apart from the most commonly used MS, there are other methods such as affinity beads for tyrosine phosphorylation, ubiquitination, acetylation, and SUMOylation-2/3 PTM that enable the trapping and identification of proteins containing these modifications [207]. There are also some specific antibodies that can be used to detect specific PTMs in proteins by immunoblot, such as the anti--peroxiredoxin-SO_3 antibody for overoxidation [208], anti-nitrotyrosine antibody for tyrosine nitration [110,209,210], as well as by immunofluorescence, like the pan-acetylation antibody [211], which allows visualizing proteins with PTMs *in vivo*. Furthermore, if a mutation can reverse the effect at the putative site of modification, then this is additional evidence to support that there is a PTM at the specific residue identified [212].

Overall, to understand the intersectional relationship of Prdx structure and their mechanism of action for whichever function requires a combinatorial approach. Indeed, it is rather uncommon that just a single technique will give information on redox state, oligomeric state, PTMs, structural architecture, etc. On the other hand, multiple experimental techniques in combination with computational methods can provide a more complete view on the structure-function dynamics and the mechanisms involved.

Table 7
Experimental techniques for investigating Prdxs: From cellular to atomic level.

Level	Techniques	Application	Reference
Cell	Optical techniques		
	Homo-FRET	Real-time monitoring of Prdx oligomerization dynamics	[116]
	FRET-based Prdx2-based H_2O_2 biosensor	H_2O_2 biosensors which show that Prdx2 undergoes a slight structural change upon oxidation	[129]
	Prdx-roGFP2 fusions	Initially designed as H_2O_2 biosensors, they can be used to gain mechanistic insight into Prdx catalysis directly in cells, including the effect of PTMs on catalysis.	[116, 130–132]
	Confocal microscopy	Visualizing the subcellular distribution and trafficking of Prdx	[31]
Protein level			
	Electron microscopy: Transmission electron microscopy (TEM), scanning electron microscopy (SEM)	Negative stain TEM is a powerful technique that was first used to characterize a heterogeneous population of Prdxs. A variety of microscopy techniques like TEM and SEM made advances in understanding Prdx oligomerization. The formation of stacked ring tubules (nanotubules) has been studied by TEM for application in nanotechnology.	[76,128, 133–141]
	Scanning probe microscopy: Atomic force microscopy (AFM), electrostatic force microscopy (EFM) and scanning tunneling microscopy (STM)	Apart from electron microscopy, also scanning probe microscopy has been used for visualizing Prdx oligomerization. For example, AFM was used to film biological molecules and examine the oligomeric state of Prdx at 10–16 frames/s, while EFM revealed the formation of nanorods containing Fe^{2+} in the central cavity as a result of the self-assembly of Prdx.	[136,139, 141,142]
	Mass spectrometry (MS): electrospray ionization MS (ESI-MS), time-resolved electrospray ionization time-of-flight MS, Hydrogen/deuterium exchange-MS (HDX-MS)	A variety of MS methods have been used to characterize Prdxs. Disulfide formation has been analyzed by ESI-MS, hyperoxidation by ESI TOF MS, and self-assemblies of Prdxs using native MS. HDX-MS relies on protein mass increases by isotopic labeling. It was used to assess the exchange rates of hydrogen for its isotope - deuterium in the C-terminal region of oxidized Prdx suggesting the exposure of this region to solvent under oxidation.	[138, 142–144]

(*continued on next page*)

Table 7 (*continued*)

Level	Techniques	Application	Reference
	Size Exclusion Chromatography (SEC)	Apparent molecular weights and oligomeric properties of Prdxs are routinely analyzed by SEC. Additionally, liquid chromatography systems can be coupled to a mass spectrometer to analyze peptides.	[80,145]
	Size exclusion chromatography coupled with multiangle light scattering (SEC-MALS)	SEC-MALS was used to monitor oligomeric state and to determine molecular weights of 2-Cys peroxiredoxins.	[146,147]
	Analytical ultra-centrifugation	Analytical ultracentrifugation can determine the different species present in solution, providing insight into whether there are dimers, rings, or tubes. Analyses of bacterial Prdxs by analytical ultracentrifugation linked the oligomeric state to the catalytic cycle, with the reduced protein forming a strong decamer and the oxidized protein tending to dissociate into dimers.	[49,75]
	Immunoblot	The oligomeric state of Prdxs such as dimer and decamer can also be analyzed by immunoblot using non-reducing and native gels.	[116,131]
In silico	Molecular dynamics (MD) simulation, Quantum mechanics/ molecular mechanics (QM/MM) simulation	MD simulations were used to predict how hyperoxidation of Prdx6 induces alteration from the dimeric to the oligomeric state. The catalytic mechanism of Prdxs was studied using QM/MM.	[148–150]
Secondary structure	Spectroscopy	Spectroscopic techniques use polarized light and interaction of light with proteins.	
	Circular dichroism (CD)	Quantitative analysis of CD spectra allows the prediction of the protein secondary structure. In Prdx studies CD is used as a complimentary technique for following the conformational as well as oligomeric changes upon nitration, (hyper)oxidation and reduction.	[111,148, 151]
	Surface-enhanced Raman scattering (SERS) spectroscopy	In SERS, the non-destructive Raman signal of adsorbed molecules is amplified on the responsive surface with high specificity. The assembly of nanostructures that use Prdx as both a bio-linker and platform for attaching molecules has been assessed by SERS in nanoprobe development for intracellular imaging.	[134]

Table 7 (*continued*)

Level	Techniques	Application	Reference
Protein shape	Scattering		
	Small angle X-ray scattering (SAXS)	SAXS has been used to confirm the toroidal nature of the oligomerization of reduced Prdx3. In combination with other methods, SAXS was applied to observe alterations of the overall Prdx structure in solution due to redox modulation.	[106,137]
	Dynamic light scattering (DLS)	DLS yields information on the size-distribution profile of molecules in solution. This can be used as a proxy to give an averaged perspective of the oligomeric state of the protein. In an early example it was shown that the oligomeric state of the Prdx is redox state dependent.	[50]
3D structure model	Atomic resolution structure model		
	X-ray crystallography	Starting from the fist X-ray structure of Prdx in 2000, the PDB contains many examples of X-ray structures of different Prdxs, mutants, monomers, dimers and oligomers, in oxidized and reduced states (Tables 1–4).	[75]
	Nuclear magnetic resonance (NMR) Spectroscopy	NMR techniques are used for the determination of the structure and dynamics of flexible biological macromolecules. The main advantage of NMR is that it provides information on proteins in solution. NMR has been used in combination with X-ray crystallography to link the oligomeric state of Prdx with their functionality. In combination with X-ray crystallography, SAXS and DLS, NMR revealed critical residues of Prdx involved in the protein-protein interactions. The conformational dynamics of the PrdxQ subgroup in both the reduced and oxidized states have been studied together with circular dichroism spectroscopy measurements. Moreover, Prdxs from various species have been assessed for the interactions with ligands in screening for fragment-based leads.	[106, 152–158]
	Cryogenic-electron microscopy (cryo-EM)	Cryo-EM has long held the promise to deliver	[5,159, 160]

(*continued on next page*)

Table 7 (*continued*)

Level	Techniques	Application	Reference
		high-resolution structure determination of biomolecules in solution. The temperature dependent structural rearrangements of reduced, 2-Cys Prdx in complex with a client protein in the center of the decamer ring was determined to 2.9 Å resolution. Large assemblies of Prdx filaments with varying lengths are particularly well suited for cryo-EM analysis. A separate study focused on cryo-EM method development and the benefits of Volta phase plates for single-particle analysis by structure determination of 257 kDa human Prdx3 dodecamers at 4.4 Å resolution.	

5. Overall insights and future perspectives

Fortunately, for the human Prdxs in general, every oligomeric state has been structurally captured and so has every oxidation state overall (meaning across several different isoforms; not for one isoform alone), except for substrate bound human Prdx. However, because it is highly likely that individual isoforms exhibit different structures for each state (i.e redox, oligomeric, etc), ideally in the future, complete structural portfolios for each isoform needs to be solved. Essentially the structural portfolio would be most complete if each oxidation state could be captured in each "conventional" oligomeric state. For example, the SH Prdx in both dimer and decameric context (or monomer, dimer context like in the case of Prdx5, an atypical, 2-Cys Prdx). This is assuming each isoform in the different subcategories oligomerizes in the same fashion. For example, because Prdx3 can crystallize in stacked decamers, can Prdx1 and Prdx2 also? These HMW oligomers have been observed for Prdx1 and Prdx2 *in vivo* [37,51], but for Prdx4 the evidence is less clear. For Prdx5 and Prdx6 so far, no decamerization or HMW structural forms have been reported.

For a full library of human Prdx structures to be completed, the structures that are required for Prdx1 are: -SOH, -SO_2, a decamer, and a stacked decamer. For Prdx2: -SO_2, a stacked decamer, and a dimer structure. Prdx3 only has the stacked 3-ring HMW, so the -SOH, SS, a single decamer, and a dimer structure are all missing. Prdx4, despite its abundant structures are available, still lacks a dimer and stacked decamer structure. Prdx5 needs a -SOH structure. Prdx6 is without an SS structure (in disulfide with a resolving partner). There is also a very pronounced demand for structures of human Prdxs in complex with binding partners involved in cell signaling. Additionally, a substrate-bound structure of a human Prdx is also vital.

For human Prdx structures, structural information for Prdxs that have PTMs or even PTM-mimicking mutations (aside from S-sulfenylation and disulfide formation, since those are included as PTMs in this analysis) are missing. From a structural and mechanistic perspective,

Table 8
High-throughput methods for the identification of Prdx interactors.

Methods	Prdx1 interactor	Prdx2 Interactor	Prdx3 Interactor	Prdx4 Interactor	Prdx5 Interactor	Prdx6 Interactor
Native PAGE – MS		CAT [161]				
IP/pulldown – MS	PIN1 [35], GDE2 [162], HDAC6 [42], p66Shc [163], APE1 [164], HBx [165]	cdB3 [166], Erp46 [167], Gardos channel [168], HDAC6 [42], PIN1 [35], VEGF-R [169], PL-D1 [170]	PIN1 [35]	PIN1 [35]	SOD1 [171] (DSP crosslinking)	Gαi3 [172], NPM [173]
2D electrophoresis – MS	TPD52 [174]	STAT3 [21]				APE1 [175]
iPOND (isolation of protein on nascent DNA) – MS		TIMELESS [34]				
Kinetic trapping – MS	TRX-1 [176]	TRX-1 [176]				
Yeast Two Hybrid Screen – co-IP	eEF1A-2 [177], Mst1&2 [37], Abl [178], c-Myc [179], MIF [180]. Omi [181]		FANCG [182], LRRK2 [183], LZK [184], LZK [185], hNek6 [185], RPK118 [186]	Prdx1 [187], TPβ [188]		STH [189], AE1 [189], Noxa1 [190]

Table 9
Methods to verify potential Prdx interactors

Methods	Prdx1 Interactor	Prdx2 Interactor	Prdx3 Interactor	Prdx4 Interactor	Prdx5 Interactors	Prdx6 Interactor
Chromatography		Stomatin [191]				
Proximity-based immunofluorescence (PLA, etc.)		ANXA2 [31]				πGST [192]
Yeast two-hybrid		PDGF-R [193]				
Co-IP/pulldown	AR [194], TLR4 [195], ASK1 [33], GSTpi-JNK complex [196], PTEN [197], FOXO3 [198], PPP3CA [199], TRAF6 [200], NF-κB [201]	STAT3 [21], tankyrase [202]		GDE2 [162]	Nrf2 [203]	Sumo1 [204], NPM [173]
Co-localization	GDE2 [162]			caspase-1 [205], GDE2 [162]	Nrf2 [203]	NPM [173]
X-ray crystallography	Srx [72]					
Co-incubation SDS-PAGE - MS				caspase-1 [205], PDI [206], PDIA6 [206], TXNDC5 [206]		

Table 10
PTMs of human Prdxs identified by high-throughput proteomics studies listed in the PhosphoSite database

Name	Residue	PTM
Prdx1	Thr^{18}, Thr^{111}, Thr^{156}, Thr^{166}, Ser^{30}, Ser^{77}, Ser^{80}, Ser^{106}, Ser^{126}, Ser^{181}, Ser^{196}, Tyr^{34}, Tyr^{116}	P
	Lys^{7}, Lys^{16}, Lys^{93}, Lys^{185}	Ac, Ub, Sm
	Lys^{35}, Lys^{37}, Lys^{68}, Lys^{109}, Lys^{136}, Lys^{168}, Lys^{178}, Lys^{192},	Ac, Ub
	Lys^{92}	Ac
	Lys^{120}, Lys^{190}	Ub
	Lys^{67}	Sm
Prdx2	Thr^{18}, Thr^{120}, Thr^{142}, Thr^{182}, Ser^{3}, Ser^{31}, Ser^{112}, Ser^{151}, Ser^{190}, Ser^{195}, Tyr^{115}, Tyr^{126}, Tyr^{193}	P
	Lys^{10}, Lys^{16}, Lys^{26}, Lys^{29}, Lys^{119}, Lys^{135}, Lys^{191}	Ac, Ub
	Lys^{34}	Ac
	Lys^{92}, Lys^{177}	Ub
Prdx3	Thr^{212}, Thr^{234}, Ser^{86}, Ser^{179}, Ser^{199}, Ser^{237}, Tyr^{71}, Tyr^{172}	P
	Lys^{196}	Ac, Ub, Sm
	Lys^{83}, Lys^{91}	Ac, Ub
	Lys^{93}, Lys^{248}	Ac
	Lys^{149}, Lys^{241}, Lys^{253}	Ub
Prdx4	Ser^{68}, Ser^{73}, Tyr^{188}, Tyr^{191}, Tyr^{266}	P
	Lys^{99}, Lys^{208}	Ac, Ub
	Lys^{78}, Lys^{102}, Lys^{263}, Lys^{265}	Ub
Prdx5	Thr^{97}, Ser^{34}, Ser^{101}, Ser^{182}	P
	Lys^{83}	Ac, Ub
	Lys^{75}, Lys^{86}, Lys^{102}, Lys^{116}, Lys^{118}, Lys^{146}, Lys^{159}	Ub
Prdx6	Thr^{44}, Thr^{130}, Ser^{32}, Ser^{83}, Ser^{146}, Ser^{186}, Tyr^{89}	P
	Lys^{56}, Lys^{63}, Lys^{182}, Lys^{209}	Ac, Ub, Sm
	Lys^{97}, Lys^{122}, Lys^{141}	Ac, Ub
	Lys^{125}, Lys^{199}	Ub, Sm
	Lys^{142}, Lys^{144}, Lys^{216}	Ac
	Lys^{84}, Lys^{200}	Ub
	Lys^{204}	Sm

P = Phosphorylation; Ac = Acetylation; Ub = Ubiquitination; Sm = SUMOylation.

Table 11
PTMs in bacterial Prdxs identified by high-throughput proteomics studies

Name	Organism	Residue	PTM	Stress	Reference
AhpC (DirA)	*Mycobacterium smegmatis* *Corynebacterium diphtheriae* *Mycobacterium tuberculosis*[#]	Cys^{61}	MSH	NaOCl	[214,215]
	Staphylococcus aureus	Cys^{168}	CoA	Diamide	[216]
	Klebsiella pneumoniae *Escherichia coli*[#]	Tyr^{157}	P		[217]
	Bacillus subtilis *Bacillus amyloliquefaciens* *Bacillus megaterium* *Staphylococcus carnosus*	Cys^{47}-Cys^{166}	S-S	NaOCl	[213]
	Escherichia coli	Lys?	Ac		[218]
YkuU[a]	*Bacillus pumilus*	Cys^{52}-Cys^{169}	S-S	NaOCl	[213]
	Bacillus pumilus	Cys^{169}	BSH	NaOCl	[213]
YgaF[a]	*Bacillus pumilus*	Cys^{45}	S-S (?)	NaOCl	[213]
Tpx	*Mycobacterium smegmatis* *Corynebacterium glutamicum* *Mycobacterium tuberculosis*[#]	Cys^{60}	MSH	NaOCl	[214]
Tpx	*Escherichia coli*	Ser^{17}, Ser^{2}, Ser^{23}, Ser^{36}, Thr^{4}, Ser^{55}, Ser^{64}, Thr^{39}	P		[219–221]
sll1621[a]	*Synechocystis* sp.	Ser^{122}, Ser^{181}	P		[222,223]

MSH = S-mycothiolation; CoA = S-CoAlation; P = phosphorylation; S-S = disulfide bond formation; Ac = acetylation; BSH = bacillithiolation.
[a] Belong to the AhpC/TSA subfamily of peroxiredoxins.

many questions on the layers and modes of Prdx regulation need to be answered. For example, all the residues listed in Table 10 are residues identified in human Prdxs via MS high-throughput methods, but they have yet to be further explored and confirmed. Their verification will determine their significance.

Similar to human Prdxs, currently there are structures available for bacterial Prdxs of several classes (Prdx1/AhpC, Tpx, BCP/PrdxQ, AhpE), oligomeric and redox states (Table 3 and 4**)**. As can be seen, so far, there have been no structures solved for bacterial representatives of the Prdx5 and Prdx6 class. However, even for the available classes, there is not a single Prdx with a complete portfolio. For example, structures of both reduced and oxidized AhpC have only been solved in the decameric and dodecameric forms, though AhpC is also known to exist as a dimer in solution [105]. As mentioned above, listing a full library of missing bacterial Prdx structures is an unsurmountable task, given the plethora of Prdxs that can be found across the multitude of prokaryotes.

Apart from those "classical" structures in different redox and oligomeric states, structures of bacterial Prdxs with PTMs are also missing, except for the oxidized forms (S-sulfenylated, S-sulfinylated and disulfide bonded, designated here as PTMs and presented in Table 6). In general, much less focus has been given to the investigation of PTMs and their influence on catalysis for bacterial Prdxs, compared to human ones. Indeed, the dbPSP (database of phosphorylation sites in prokaryotes - http://dbpsp.biocuckoo.cn) only returns a handful of publications when giving bacterial Prdxs as an input, and all those are from high-throughput studies (Table 11), which also have yet to be validated and their role in Prdx function determined. Information on other PTMs of bacterial Prdxs can be extracted from publications documenting the results of high-throughput studies, in which redox proteomics, MS, and immunoblotting are used to find proteins harboring a specific modification after exposure of bacteria to oxidative stress, such as sodium hypochlorite [213]. Due to the bias of this experimental setup to redox modifications, most PTMs of bacterial Prdxs are reported for Cys residues (mostly the active site, peroxidatic Cys), and represent either the direct product of oxidation, or part of the reductive cycle (Table 11). Our literature search only yielded one example of acetylation of a bacterial Prdx, AhpC, again with an unexplored role. Therefore, identifying PTMs other than those occurring on the catalytic Cys and establishing their role in catalysis of the Prdx with a more systematic approach, is definitely an avenue to follow. We would also like to point out that a curated database of bacterial Prdx (and other protein) PTMs should be set up, or these PTMs should be added to the UniProt entries.

To summarize, in the coming years, we expect that the solving of missing structures of Prdxs mentioned above, the elucidation of the role specific PTMs play in modulating Prdx function and PPIs and the validation of the many potential interactors yielded by high-throughput studies will be the primary lines of research in the field.

Regarding obtaining the missing structures, so far, the workhorse technique for solving the atomic structures of Prdxs has been X-ray crystallography and to some extent NMR, and these techniques are still expected to contribute to Prdx research in the future. This is especially true as laboratory automation and use of high-throughput screening is reducing the amount of protein needed for crystallization while remote access and automated sample changers at synchrotrons are speeding up data collection from protein crystals. Nevertheless, there are a number of exciting advancements in other techniques that will increase our understanding of Prdxs at atomic resolution.

Indeed, cryo-EM is becoming more and more popular which is reflected in the rising number of protein structures deposited in the PDB or Electron Microscopy Data Bank (EMDB) [224]. Micro-Electron diffraction (MicroED) is gaining attention as it can be used to determine

high-resolution protein structures by electron crystallography of three-dimensional crystals in an electron microscope [225]. Compared to X-ray crystallography, MicroED additionally provides valuable information on the charged state of the protein because the diffraction patterns are generated with charged particles (electrons) rather than X-rays. Neutron diffraction is one of the few approaches so far that allows to locate mobile or highly polarized H atoms and protons, once the key bottleneck of obtaining suitable diffraction quality crystals is overcome [226]. This technique could therefore allow us to better visualize rearrangements of the H-network of Prdx during the peroxidatic cycle, perhaps revealing molecular details that were missed by X-ray crystallography. It could also be used to obtain the lacking human structures of Prdx bound with H_2O_2. Of note, an important aspect regarding these biophysical techniques is their availability and accessibility to new users. To this end, large-scale research facilities offer various users' programs, where experts provide support in planning and preparation of experiments, data collection, and data analysis. Hence, it is likely that these techniques that so far have not been used to study Prdxs will join the repertoire of methods in the field.

The structural portfolios of Prdxs in different redox and oligomerization states could be enhanced by dynamic information, especially in the context of PTMs and PPIs. This would be particularly relevant, for instance, when Prdx HMW oligomer formation triggers cell cycle checkpoints [51]. This suggests that the HMW oligomers could be detected by the cells and interpreted as stress signals, but there are also other examples where the HMW forms behave as chaperones and the HMW formation is caused by phosphorylation [36]. Thus, the dynamics of oligomerization states are important to query further in order to understand the delineation and time frames of the putative roles for HMW Prdx oligomers. For this purpose, nanotechnology techniques such as high-speed atomic force microscopy (HS-AFM), (which has already been used for Prdx (Table 7)) can be employed. They would enable us to visualize and even manipulate (e.g. with optical tweezers) Prdx molecules in dynamic action at high spatiotemporal resolution [139].

As discussed above, a big question in the Prdx field remains the PPIs they are involved in. As outlined in Table 8, there are several methods available for the generation of lists of interactor candidates by high-throughput approaches, but the true challenge lies in knowing how to properly select the real binding partners among them for further validation. An accurate prediction technique for PPIs would therefore help to streamline the process of selecting potential binding partners. This could be accomplished by the many protein-protein docking simulators that have been developed recently. The HADDOCK server [227] (http://milou.science.uu.nl/services/HADDOCK2.2/) is currently one of the widely-used simulators. Using the existing structure information of two proteins as an input, the protein-protein docking simulator is able to give a relatively accurate prediction on whether there is a binding site between them. However, it should be kept in mind that most of the time those predictions are focused on direct PPI and will yield no results if the two proteins are indirect interactors within a protein complex, which is often the case when PPIs are detected by high-throughput methods. Unfortunately, there are only very limited tools on protein complex prediction currently available, such as one that relies on the assumption that proteins that do not interact directly, yet share interaction partners, can be part of the same complex [228]. Other computational techniques, such as molecular dynamic simulations could also be employed to make new predictions about PPIs [148]. These could become especially useful, for example, when investigating the influence of certain PTMs on PPIs Prdxs are involved in. However, it should be kept in mind that computational techniques have rather a predictive nature and should be cross-validated in a wet lab experimental set-up.

Ideally, Prdx redox-relays and other PPIs should be confirmed and characterized on several levels: the structural level (e.g. using methods outlined in this section), a biochemical one, i.e. the determination of stoichiometry of complex formation, as well as in cells (Table 9). While X-ray crystallography has been used in the past for studying complexes, stabilizing complexes for crystallization is a notable challenge and requires such approaches as chemical crosslinking and Nanobody technology [229]. An emerging technique that is simpler and less time-consuming is Mass Photometry (MP), which uses light scattering to detect and measure the molecular mass of individual unlabeled biomolecules that had adsorbed from solution to a glass surface in biologically relevant environments. The big advantage of this method is that it allows the direct detection of protein complex formation in solution [230], and therefore holds particular promise for studying Prdx redox-relays and other PPIs.

Yet another outstanding question in the Prdx field that can only be addressed in cells is whether their subcellular localization is influenced by PTMs or PPIs. For answering this question, techniques for detecting PPI or PTMs will have to be utilized in combination with immunolabeling and fluorescence microscopy. Finally, despite everything we know on Prdxs summarized in this review, we still do not have a clear picture on their role in physiology, and especially signaling. To investigate this, the obvious approach is to knock-down Prdx in the cell of interest. Fortunately, modern techniques including CRISPR/Cas9, haploid cells [31,32] and Trim-Away – a technique that exploits the protein TRIM21 to directly and rapidly deplete specific proteins in cells [231] – allows this to be done in most labs working with cell culture without resorting to mice.

We would like to reiterate that the missing structures and outstanding questions outlined above, such as the role of specific PTMs in modulating Prdx function, can only be fully answered using a combination of techniques. Even though here we divided the techniques into "atom level", "cell level", "*in vitro*" and "*in vivo*", in reality, with the development of new techniques the classification of them, just as Prdxs themselves, is becoming difficult. A good example is cryo-electron tomography, which brings molecular-level views into cellular biology [232]. This opens the possibility to study Prdxs *in situ* with increased resolution and to discern how the Prdx intersectional functions are controlled and switched, as well as shed light on the mechanistic details surrounding their versatility.

In conclusion, we are entering a new era of integrative structural biology that allows us to 'see' the Prdx structure on multiple scales, from atom to organism and vice versa. The time has never been better to finally understand the intersectional factors of Prdxs (structure, redox state, PPI, PTMs, localization, etc) and how they influence the many key roles Prdxs play. Ultimately this information will give us a clearer view of the power Prdxs exert on cellular (patho)physiology through their involvement in both stress and non-stress signaling.

Funding

This work was funded with a VIB grant (to J.M.), and the Research Foundation-Flanders–Fonds de la Recherche Scientifique Excellence of Science project no. 30829584 (to J.M). Ting L. was supported with a Chinese Scholarship Council grant (File No. 201707650018).

Declaration of competing interest

The authors declare no competing interests.

References

[1] A. Hall, P.A. Karplus, L.B. Poole, Typical 2-Cys peroxiredoxins–structures, mechanisms and functions, FEBS J. 276 (2009) 2469–2477.
[2] Z.A. Wood, L.B. Poole, P.A. Karplus, Peroxiredoxin evolution and the regulation of hydrogen peroxide signaling, Science 300 (2003) 650–653.
[3] Z.A. Wood, E. Schröder, J. Robin Harris, L.B. Poole, Structure, mechanism and regulation of peroxiredoxins, Trends Biochem. Sci. 28 (2003) 32–40.
[4] S.G. Rhee, H.A. Woo, Multiple functions of 2-Cys peroxiredoxins, I and II, and their regulations via post-translational modifications, Free Radic. Biol. Med. 152 (2020) 107–115.
[5] F. Teixeira, E. Tse, H. Castro, K.A.T. Makepeace, B.A. Meinen, C.H. Borchers, L. B. Poole, J.C. Bardwell, A.M. Tomas, D.R. Southworth, U. Jakob, Chaperone

activation and client binding of a 2-cysteine peroxiredoxin, Nat. Commun. 10 (2019) 659.
[6] A. Hall, K. Nelson, L.B. Poole, P.A. Karplus, Structure-based insights into the catalytic power and conformational dexterity of peroxiredoxins, Antioxidants Redox Signal. 15 (2011) 795–815.
[7] C.C. Winterbourn, The biological chemistry of hydrogen peroxide, Methods Enzymol. 528 (2013) 3–25.
[8] C.C. Winterbourn, Reconciling the chemistry and biology of reactive oxygen species, Nat. Chem. Biol. 4 (2008) 278–286.
[9] C.C. Winterbourn, M.B. Hampton, Redox biology: signaling via a peroxiredoxin sensor, Nat. Chem. Biol. 11 (2015) 5–6.
[10] H.Z. Chae, T.B. Uhm, S.G. Rhee, Dimerization of thiol-specific antioxidant and the essential role of cysteine 47, Proc. Natl. Acad. Sci. U. S. A. 91 (1994) 7022–7026.
[11] H.Z. Chae, S.J. Chung, S.G. Rhee, Thioredoxin-dependent peroxide reductase from yeast, J. Biol. Chem. 269 (1994) 27670–27678.
[12] H. Kawagishi, T. Finkel, Unraveling the truth about antioxidants: ROS and disease: finding the right balance, Nat. Med. 20 (2014) 711–713.
[13] K. Kim, I.H. Kim, K.Y. Lee, S.G. Rhee, E.R. Stadtman, The isolation and purification of a specific "protector" protein which inhibits enzyme inactivation by a thiol/Fe(III)/O2 mixed-function oxidation system, J. Biol. Chem. 263 (1988) 4704–4711.
[14] R. Bryk, P. Griffin, C. Nathan, Peroxynitrite reductase activity of bacterial peroxiredoxins, Nature 407 (2000) 211–215.
[15] S.G. Rhee, H.A. Woo, I.S. Kil, S.H. Bae, Peroxiredoxin functions as a peroxidase and a regulator and sensor of local peroxides, J. Biol. Chem. 287 (2012) 4403–4410.
[16] S.G. Rhee, Cell signaling. H2O2, a necessary evil for cell signaling, Science 312 (2006) 1882–1883.
[17] H. Sies, Hydrogen peroxide as a central redox signaling molecule in physiological oxidative stress: oxidative eustress, Redox Biol. 11 (2017) 613–619.
[18] H. Sies, Role of metabolic H2O2 generation: redox signaling and oxidative stress, J. Biol. Chem. 289 (2014) 8735–8741.
[19] H. Sies, D.P. Jones, Reactive oxygen species (ROS) as pleiotropic physiological signalling agents, Nat. Rev. Mol. Cell Biol. 21 (2020) 363–383.
[20] R.M. Jarvis, S.M. Hughes, E.C. Ledgerwood, Peroxiredoxin 1 functions as a signal peroxidase to receive, transduce, and transmit peroxide signals in mammalian cells, Free Radic. Biol. Med. 53 (2012) 1522–1530.
[21] M.C. Sobotta, W. Liou, S. Stöcker, D. Talwar, M. Oehler, T. Ruppert, A.N. Scharf, T.P. Dick, Peroxiredoxin-2 and STAT3 form a redox relay for H2O2 signaling, Nat. Chem. Biol. 11 (2015) 64–70.
[22] S. Stöcker, K. Van Laer, A. Mijuskovic, T.P. Dick, The conundrum of hydrogen peroxide signaling and the emerging role of peroxiredoxins as redox relay hubs, Antioxidants Redox Signal. 28 (2018) 558–573.
[23] D.E. Fomenko, A. Koc, N. Agisheva, M. Jacobsen, A. Kaya, M. Malinouski, J. C. Rutherford, K.L. Siu, D.Y. Jin, D.R. Winge, V.N. Gladyshev, Thiol peroxidases mediate specific genome-wide regulation of gene expression in response to hydrogen peroxide, Proc. Natl. Acad. Sci. U. S. A. 108 (2011) 2729–2734.
[24] N. Brandes, S. Schmitt, U. Jakob, Thiol-based redox switches in eukaryotic proteins, Antioxidants Redox Signal. 11 (2009) 997–1014.
[25] S. Messina, G. De Simone, P. Ascenzi, Cysteine-based regulation of redox-sensitive Ras small GTPases, Redox Biol. 26 (2019) 101282.
[26] B. Pedre, D. Young, D. Charlier, A. Mourenza, L.A. Rosado, L. Marcos-Pascual, K. Wahni, E. Martens, G.d.l.R. A, V.V. Belousov, L.M. Mateos, J. Messens, Structural snapshots of OxyR reveal the peroxidatic mechanism of H2O2 sensing, Proc. Natl. Acad. Sci. U. S. A. 115 (2018) E11623–E11632.
[27] S. Barranco-Medina, J.J. Lazaro, K.J. Dietz, The oligomeric conformation of peroxiredoxins links redox state to function, FEBS Lett. 583 (2009) 1809–1816.
[28] W. Sun, L. Dai, H. Yu, B. Puspita, T. Zhao, F. Li, J.L. Tan, Y.T. Lim, M.W. Chen, R. M. Sobota, D.G. Tenen, N. Prabhu, P. Nordlund, Monitoring structural modulation of redox-sensitive proteins in cells with MS-CETSA, Redox Biol. 24 (2019) 101168.
[29] C. Klomsiri, P.A. Karplus, L.B. Poole, Cysteine-based redox switches in enzymes, Antioxidants Redox Signal. 14 (2011) 1065–1077.
[30] K. Skryhan, J.A. Cuesta-Seijo, M.M. Nielsen, L. Marri, S.B. Mellor, M.A. Glaring, P. E. Jensen, M.M. Palcic, A. Blennow, The role of cysteine residues in redox regulation and protein stability of Arabidopsis thaliana starch synthase 1, PLoS One 10 (2015), e0136997.
[31] D. Talwar, J. Messens, T.P. Dick, A role for annexin A2 in scaffolding the peroxiredoxin 2-STAT3 redox relay complex, Nat. Commun. 11 (2020) 4512.
[32] S. Stöcker, M. Maurer, T. Ruppert, T.P. Dick, A role for 2-Cys peroxiredoxins in facilitating cytosolic protein thiol oxidation, Nat. Chem. Biol. 14 (2018) 148–155.
[33] S.Y. Kim, T.J. Kim, K.Y. Lee, A novel function of peroxiredoxin 1 (Prx-1) in apoptosis signal-regulating kinase 1 (ASK1)-mediated signaling pathway, FEBS Lett. 582 (2008) 1913–1918.
[34] K. Somyajit, R. Gupta, H. Sedlackova, K.J. Neelsen, F. Ochs, M.B. Rask, C. Choudhary, J. Lukas, Redox-sensitive alteration of replisome architecture safeguards genome integrity, Science 358 (2017) 797–802.
[35] K.L. Chu, Q.J. Lew, V. Rajasegaran, J.T. Kung, L. Zheng, Q. Yang, R. Shaw, N. Cheong, Y.C. Liou, S.H. Chao, Regulation of PRDX1 peroxidase activity by Pin1, Cell Cycle 12 (2013) 944–952.
[36] H.H. Jang, S.Y. Kim, S.K. Park, H.S. Jeon, Y.M. Lee, J.H. Jung, S.Y. Lee, H.B. Chae, Y.J. Jung, K.O. Lee, C.O. Lim, W.S. Chung, J.D. Bahk, D.J. Yun, M.J. Cho, S.Y. Lee, Phosphorylation and concomitant structural changes in human 2-Cys peroxiredoxin isotype I differentially regulate its peroxidase and molecular chaperone functions, FEBS Lett. 580 (2006) 351–355.
[37] S.J. Rawat, C.L. Creasy, J.R. Peterson, J. Chernoff, The tumor suppressor Mst1 promotes changes in the cellular redox state by phosphorylation and inactivation of peroxiredoxin-1 protein, J. Biol. Chem. 288 (2013) 8762–8771.
[38] H.A. Woo, S.H. Yim, D.H. Shin, D. Kang, D.Y. Yu, S.G. Rhee, Inactivation of peroxiredoxin I by phosphorylation allows localized H(2)O(2) accumulation for cell signaling, Cell 140 (2010) 517–528.
[39] T.A. Zykova, F. Zhu, T.I. Vakorina, J. Zhang, L.A. Higgins, D.V. Urusova, A. M. Bode, Z. Dong, T-LAK cell-originated protein kinase (TOPK) phosphorylation of Prx1 at Ser-32 prevents UVB-induced apoptosis in RPMI7951 melanoma cells through the regulation of Prx1 peroxidase activity, J. Biol. Chem. 285 (2010) 29138–29146.
[40] M.C. Chung, F. Alem, S.G. Hamer, A. Narayanan, K. Shatalin, C. Bailey, E. Nudler, R.M. Hakami, S-nitrosylation of peroxiredoxin 1 contributes to viability of lung epithelial cells during Bacillus anthracis infection, Biochim. Biophys. Acta Gen. Subj. 1861 (2017) 3019–3029.
[41] Y. Pan, J.H. Jin, Y. Yu, J. Wang, Significant enhancement of hPrx1 chaperone activity through lysine acetylation, Chembiochem 15 (2014) 1773–1776.
[42] R.B. Parmigiani, W.S. Xu, G. Venta-Perez, H. Erdjument-Bromage, M. Yaneva, P. Tempst, P.A. Marks, HDAC6 is a specific deacetylase of peroxiredoxins and is involved in redox regulation, Proc. Natl. Acad. Sci. U. S. A. 105 (2008) 9633–9638.
[43] D. Qu, J. Rashidian, M.P. Mount, H. Aleyasin, M. Parsanejad, A. Lira, E. Haque, Y. Zhang, S. Callaghan, M. Daigle, M.W. Rousseaux, R.S. Slack, P.R. Albert, I. Vincent, J.M. Woulfe, D.S. Park, Role of Cdk5-mediated phosphorylation of Prx2 in MPTP toxicity and Parkinson's disease, Neuron 55 (2007) 37–52.
[44] R.R. Tao, H. Wang, L.J. Hong, J.Y. Huang, Y.M. Lu, M.H. Liao, W.F. Ye, N.N. Lu, D.Y. Zhu, Q. Huang, K. Fukunaga, Y.J. Lou, I. Shoji, C.S. Wilcox, E.Y. Lai, F. Han, Nitrosative stress induces peroxiredoxin 1 ubiquitination during ischemic insult via E6AP activation in endothelial cells both in vitro and in vivo, Antioxidants Redox Signal. 21 (2014) 1–16.
[45] Z. Wang, R. Sun, G. Wang, Z. Chen, Y. Li, Y. Zhao, D. Liu, H. Zhao, F. Zhang, J. Yao, X. Tian, SIRT3-mediated deacetylation of PRDX3 alleviates mitochondrial oxidative damage and apoptosis induced by intestinal ischemia/reperfusion injury, Redox Biol. 28 (2020) 101343.
[46] Y. Wu, S.I. Feinstein, Y. Manevich, I. Chowdhury, J.H. Pak, A. Kazi, C. Dodia, D. W. Speicher, A.B. Fisher, Mitogen-activated protein kinase-mediated phosphorylation of peroxiredoxin 6 regulates its phospholipase A(2) activity, Biochem. J. 419 (2009) 669–679.
[47] Y. Zhang, C. Sun, G. Xiao, H. Shan, L. Tang, Y. Yi, W. Yu, Y. Gu, S-nitrosylation of the Peroxiredoxin-2 promotes S-nitrosoglutathione-mediated lung cancer cells apoptosis via AMPK-SIRT1 pathway, Cell Death Dis. 10 (2019) 329.
[48] S. Cho, K.W. Crenshaw, L. McCall, Toward a field of intersectionality studies: theory, applications, and praxis. Signs, J. Women Cult. Soc. 38 (2013) 785–810.
[49] D. Parsonage, D.S. Youngblood, G.N. Sarma, Z.A. Wood, P.A. Karplus, L.B. Poole, Analysis of the link between enzymatic activity and oligomeric state in AhpC, a bacterial peroxiredoxin, Biochemistry 44 (2005) 10583–10592.
[50] Z.A. Wood, L.B. Poole, R.R. Hantgan, P.A. Karplus, Dimers to doughnuts: redox-sensitive oligomerization of 2-cysteine peroxiredoxins, Biochemistry 41 (2002) 5493–5504.
[51] T.J. Phalen, K. Weirather, P.B. Deming, V. Anathy, A.K. Howe, A. van der Vliet, T. J. Jonsson, L.B. Poole, N.H. Heintz, Oxidation state governs structural transitions in peroxiredoxin II that correlate with cell cycle arrest and recovery, J. Cell Biol. 175 (2006) 779–789.
[52] F. Saccoccia, P. Di Micco, G. Boumis, M. Brunori, I. Koutris, A.E. Miele, V. Morea, P. Sriratana, D.L. Williams, A. Bellelli, F. Angelucci, Moonlighting by different stressors: crystal structure of the chaperone species of a 2-Cys peroxiredoxin, Structure 20 (2012) 429–439.
[53] J.P. Declercq, C. Evrard, A. Clippe, D.V. Stricht, A. Bernard, B. Knoops, Crystal structure of human peroxiredoxin 5, a novel type of mammalian peroxiredoxin at 1.5 A resolution, J. Mol. Biol. 311 (2001) 751–759.
[54] K.J. Nelson, A. Perkins, A.E.D. Van Swearingen, S. Hartman, A.E. Brereton, D. Parsonage, F.R. Salsbury Jr., P.A. Karplus, L.B. Poole, Experimentally dissecting the origins of peroxiredoxin catalysis, Antioxidants Redox Signal. 28 (2018) 521–536.
[55] A. Perkins, K.J. Nelson, J.R. Williams, D. Parsonage, L.B. Poole, P.A. Karplus, The sensitive balance between the fully folded and locally unfolded conformations of a model peroxiredoxin, Biochemistry 52 (2013) 8708–8721.
[56] A. Perkins, D. Parsonage, K.J. Nelson, O.M. Ogba, P.H. Cheong, L.B. Poole, P. A. Karplus, Peroxiredoxin catalysis at atomic resolution, Structure 24 (2016) 1668–1678.
[57] L.B. Poole, K.J. Nelson, Distribution and features of the six classes of peroxiredoxins, Mol Cells 39 (2016) 53–59.
[58] Y. Manevich, A.B. Fisher, Peroxiredoxin 6, a 1-Cys peroxiredoxin, functions in antioxidant defense and lung phospholipid metabolism, Free Radic. Biol. Med. 38 (2005) 1422–1432.
[59] J.A. Bolduc, K.J. Nelson, A.C. Haynes, J. Lee, J.A. Reisz, A.H. Graff, J. E. Clodfelter, D. Parsonage, L.B. Poole, C.M. Furdui, W.T. Lowther, Novel hyperoxidation resistance motifs in 2-Cys peroxiredoxins, J. Biol. Chem. 293 (2018) 11901–11912.
[60] A.F. Harper, J.B. Leuthaeuser, P.C. Babbitt, J.H. Morris, T.E. Ferrin, L.B. Poole, J. S. Fetrow, An atlas of peroxiredoxins created using an active site profile-based approach to functionally relevant clustering of proteins, PLoS Comput. Biol. 13 (2017), e1005284.
[61] K.J. Nelson, D. Parsonage, A. Hall, P.A. Karplus, L.B. Poole, Cysteine pK(a) values for the bacterial peroxiredoxin AhpC, Biochemistry 47 (2008) 12860–12868.

[62] R. Ogusucu, D. Rettori, D.C. Munhoz, L.E. Netto, O. Augusto, Reactions of yeast thioredoxin peroxidases I and II with hydrogen peroxide and peroxynitrite: rate constants by competitive kinetics, Free Radic. Biol. Med. 42 (2007) 326–334.

[63] M. Hugo, L. Turell, B. Manta, H. Botti, G. Monteiro, L.E. Netto, B. Alvarez, R. Radi, M. Trujillo, Thiol and sulfenic acid oxidation of AhpE, the one-cysteine peroxiredoxin from Mycobacterium tuberculosis: kinetics, acidity constants, and conformational dynamics, Biochemistry 48 (2009) 9416–9426.

[64] A.V. Peskin, F.M. Low, L.N. Paton, G.J. Maghzal, M.B. Hampton, C. C. Winterbourn, The high reactivity of peroxiredoxin 2 with H(2)O(2) is not reflected in its reaction with other oxidants and thiol reagents, J. Biol. Chem. 282 (2007) 11885–11892.

[65] M. Trujillo, G. Ferrer-Sueta, L. Thomson, L. Flohe, R. Radi, Kinetics of peroxiredoxins and their role in the decomposition of peroxynitrite, Subcell. Biochem. 44 (2007) 83–113.

[66] J.C. Toledo Jr., R. Audi, R. Ogusucu, G. Monteiro, L.E. Netto, O. Augusto, Horseradish peroxidase compound I as a tool to investigate reactive protein-cysteine residues: from quantification to kinetics, Free Radic. Biol. Med. 50 (2011) 1032–1038.

[67] D. Young, B. Pedre, D. Ezerina, B. De Smet, A. Lewandowska, M.A. Tossounian, N. Bodra, J. Huang, L. Astolfi Rosado, F. Van Breusegem, J. Messens, Protein promiscuity in H2O2 signaling, Antioxidants Redox Signal. 30 (2019) 1285–1324.

[68] T. Nakamura, Y. Kado, T. Yamaguchi, H. Matsumura, K. Ishikawa, T. Inoue, Crystal structure of peroxiredoxin from Aeropyrum pernix K1 complexed with its substrate, hydrogen peroxide, J. Biochem. 147 (2010) 109–115.

[69] X. Wang, L. Wang, X. Wang, F. Sun, C.C. Wang, Structural insights into the peroxidase activity and inactivation of human peroxiredoxin 4, Biochem. J. 441 (2012) 113–118.

[70] Z. Cao, T.J. Tavender, A.W. Roszak, R.J. Cogdell, N.J. Bulleid, Crystal structure of reduced and of oxidized peroxiredoxin IV enzyme reveals a stable oxidized decamer and a non-disulfide-bonded intermediate in the catalytic cycle, J. Biol. Chem. 286 (2011) 42257–42266.

[71] K.H. Kim, W. Lee, E.E. Kim, Crystal structures of human peroxiredoxin 6 in different oxidation states, Biochem. Biophys. Res. Commun. 477 (2016) 717–722.

[72] T.J. Jonsson, L.C. Johnson, W.T. Lowther, Structure of the sulphiredoxin-peroxiredoxin complex reveals an essential repair embrace, Nature 451 (2008) 98–101.

[73] T.J. Jonsson, L.C. Johnson, W.T. Lowther, Protein engineering of the quaternary sulfiredoxin.peroxiredoxin enzyme.substrate complex reveals the molecular basis for cysteine sulfinic acid phosphorylation, J. Biol. Chem. 284 (2009) 33305–33310.

[74] K.J. Cho, Y. Park, T. Khan, J.-H. Lee, S. Kim, J.H. Seok, Y.B. Chung, A.E. Cho, Y. Choi, T.-S. Chang, K.H. Kim, Crystal structure of dimeric human peroxiredoxin-1 C83S mutant, Bull. Kor. Chem. Soc. 36 (2015) 1543–1545.

[75] E. Schröder, J.A. Littlechild, A.A. Lebedev, N. Errington, A.A. Vagin, M.N. Isupov, Crystal structure of decameric 2-Cys peroxiredoxin from human erythrocytes at 1.7 A resolution, Structure 8 (2000) 605–615.

[76] N.A. Yewdall, H. Venugopal, A. Desfosses, V. Abrishami, Y. Yosaatmadja, M. B. Hampton, J.A. Gerrard, D.C. Goldstone, A.K. Mitra, M. Radjainia, Structures of human peroxiredoxin 3 suggest self-chaperoning assembly that maintains catalytic state, Structure 24 (2016) 1120–1129.

[77] Y. Sato, R. Kojima, M. Okumura, M. Hagiwara, S. Masui, K. Maegawa, M. Saiki, T. Horibe, M. Suzuki, K. Inaba, Synergistic cooperation of PDI family members in peroxiredoxin 4-driven oxidative protein folding, Sci. Rep. 3 (2013) 2456.

[78] R. Kojima, M. Okumura, S. Masui, S. Kanemura, M. Inoue, M. Saiki, H. Yamaguchi, T. Hikima, M. Suzuki, S. Akiyama, K. Inaba, Radically different thioredoxin domain arrangement of ERp46, an efficient disulfide bond introducer of the mammalian PDI family, Structure 22 (2014) 431–443.

[79] K. Yang, D.F. Li, X. Wang, J. Liang, R. Sitia, C.C. Wang, X. Wang, Crystal structure of the ERp44-peroxiredoxin 4 complex reveals the molecular mechanisms of thiol-mediated protein retention, Structure 24 (2016) 1755–1765.

[80] A.R. Parker, P.N. Petluru, V.L. Nienaber, J. Badger, B.D. Leverett, K. Jair, V. Sridhar, C. Logan, P.Y. Ayala, H. Kochat, F.H. Hausheer, Cysteine specific targeting of the functionally distinct peroxiredoxin and glutaredoxin proteins by the investigational disulfide BNP7787, Molecules 20 (2015) 4928–4950.

[81] A. Smeets, C. Marchand, D. Linard, B. Knoops, J.P. Declercq, The crystal structures of oxidized forms of human peroxiredoxin 5 with an intramolecular disulfide bond confirm the proposed enzymatic mechanism for atypical 2-Cys peroxiredoxins, Arch. Biochem. Biophys. 477 (2008) 98–104.

[82] A. Hall, D. Parsonage, L.B. Poole, P.A. Karplus, Structural evidence that peroxiredoxin catalytic power is based on transition-state stabilization, J. Mol. Biol. 402 (2010) 194–209.

[83] C. Aguirre, T. ten Brink, J.F. Guichou, O. Cala, I. Krimm, Comparing binding modes of analogous fragments using NMR in fragment-based drug design: application to PRDX5, PLoS One 9 (2014), e102300.

[84] C. Evrard, A. Capron, C. Marchand, A. Clippe, R. Wattiez, P. Soumillion, B. Knoops, J.P. Declercq, Crystal structure of a dimeric oxidized form of human peroxiredoxin 5, J. Mol. Biol. 337 (2004) 1079–1090.

[85] C. Evrard, A. Smeets, B. Knoops, J.-P. Declercq, Crystal structure of the C47S mutant of human peroxiredoxin 5, J. Chem. Crystallogr. 34 (2004) 553–558.

[86] H.J. Choi, S.W. Kang, C.H. Yang, S.G. Rhee, S.E. Ryu, Crystal structure of a novel human peroxidase enzyme at 2.0 A resolution, Nat. Struct. Biol. 5 (1998) 400–406.

[87] N. Kamariah, M.F. Sek, B. Eisenhaber, F. Eisenhaber, G. Gruber, Transition steps in peroxide reduction and a molecular switch for peroxide robustness of prokaryotic peroxiredoxins, Sci. Rep. 6 (2016) 37610.

[88] A. Pan, A.M. Balakrishna, W. Nartey, A. Kohlmeier, P.V. Dip, S. Bhushan, G. Gruber, Atomic structure and enzymatic insights into the vancomycin-resistant Enterococcus faecalis (V583) alkylhydroperoxide reductase subunit C, Free Radic. Biol. Med. 115 (2018) 252–265.

[89] S.J. Kim, J.R. Woo, Y.S. Hwang, D.G. Jeong, D.H. Shin, K. Kim, S.E. Ryu, The tetrameric structure of Haemophilus influenza hybrid Prx5 reveals interactions between electron donor and acceptor proteins, J. Biol. Chem. 278 (2003) 10790–10798.

[90] S. Li, N.A. Peterson, M.Y. Kim, C.Y. Kim, L.W. Hung, M. Yu, T. Lekin, B. W. Segelke, J.S. Lott, E.N. Baker, Crystal structure of AhpE from Mycobacterium tuberculosis, a 1-cys peroxiredoxin, J. Mol. Biol. 346 (2005) 1035–1046.

[91] L.A. van Bergen, M. Alonso, A. Pallo, L. Nilsson, F. De Proft, J. Messens, Revisiting sulfur H-bonds in proteins: the example of peroxiredoxin AhpE, Sci. Rep. 6 (2016) 30369.

[92] B. Pedre, L.A. van Bergen, A. Pallo, L.A. Rosado, V.T. Dufe, I.V. Molle, K. Wahni, H. Erdogan, M. Alonso, F.D. Proft, J. Messens, The active site architecture in peroxiredoxins: a case study on Mycobacterium tuberculosis AhpE, Chem. Commun. 52 (2016) 10293–10296.

[93] M. Stehr, H.J. Hecht, T. Jager, L. Flohe, M. Singh, Structure of the inactive variant C60S of Mycobacterium tuberculosis thiol peroxidase, Acta Crystallogr. D Biol. Crystallogr. 62 (2006) 563–567.

[94] M. Li, J. Wang, W. Xu, Y. Wang, M. Zhang, M. Wang, Crystal structure of Akkermansia muciniphila peroxiredoxin reveals a novel regulatory mechanism of typical 2-Cys Prxs by a distinct loop, FEBS Lett. 594 (2020) 1550–1563.

[95] J. Ahn, K.K. Jang, I. Jo, H. Nurhasni, J.G. Lim, J.W. Yoo, S.H. Choi, N.C. Ha, Crystal structure of peroxiredoxin 3 from Vibrio vulnificus and its implications for scavenging peroxides and nitric oxide, IUCrJ 5 (2018) 82–92.

[96] S.J. Liao, C.Y. Yang, K.H. Chin, A.H. Wang, S.H. Chou, Insights into the alkyl peroxide reduction pathway of Xanthomonas campestris bacterioferritin comigratory protein from the trapped intermediate-ligand complex structures, J. Mol. Biol. 390 (2009) 951–966.

[97] A. Hall, B. Sankaran, L.B. Poole, P.A. Karplus, Structural changes common to catalysis in the Tpx peroxiredoxin subfamily, J. Mol. Biol. 393 (2009) 867–881.

[98] K.S. Beckham, O. Byron, A.J. Roe, M. Gabrielsen, The structure of an orthorhombic crystal form of a 'forced reduced' thiol peroxidase reveals lattice formation aided by the presence of the affinity tag, Acta Crystallogr. Sect. F Struct. Biol. Cryst. Commun. 68 (2012) 522–526.

[99] M. Gabrielsen, K.S. Beckham, V.A. Feher, C.E. Zetterstrom, D. Wang, S. Muller, M. Elofsson, R.E. Amaro, O. Byron, A.J. Roe, Structural characterisation of Tpx from Yersinia pseudotuberculosis reveals insights into the binding of salicylidene acylhydrazide compounds, PLoS One 7 (2012), e32217.

[100] P.V. Dip, N. Kamariah, M.S. Subramanian Manimekalai, W. Nartey, A. M. Balakrishna, F. Eisenhaber, B. Eisenhaber, G. Gruber, Structure, mechanism and ensemble formation of the alkylhydroperoxide reductase subunits AhpC and AhpF from Escherichia coli, Acta Crystallogr. D Biol. Crystallogr. 70 (2014) 2848–2862.

[101] P.V. Dip, N. Kamariah, W. Nartey, C. Beushausen, V.A. Kostyuchenko, T.S. Ng, S. M. Lok, W.G. Saw, F. Eisenhaber, B. Eisenhaber, G. Gruber, Key roles of the Escherichia coli AhpC C-terminus in assembly and catalysis of alkylhydroperoxide reductase, an enzyme essential for the alleviation of oxidative stress, Biochim. Biophys. Acta 1837 (2014) 1932–1943.

[102] J. Choi, S. Choi, J. Choi, M.K. Cha, I.H. Kim, W. Shin, Crystal structure of Escherichia coli thiol peroxidase in the oxidized state: insights into intramolecular disulfide formation and substrate binding in atypical 2-Cys peroxiredoxins, J. Biol. Chem. 278 (2003) 49478–49486.

[103] W. Liu, A. Liu, H. Gao, Q. Wang, L. Wang, E. Warkentin, Z. Rao, H. Michel, G. Peng, Structural properties of the peroxiredoxin AhpC2 from the hyperthermophilic eubacterium Aquifex aeolicus, Biochim. Biophys. Acta Gen. Subj. 1862 (2018) 2797–2805.

[104] K. Kitano, A. Kita, T. Hakoshima, Y. Niimura, K. Miki, Crystal structure of decameric peroxiredoxin (AhpC) from Amphibacillus xylanus, Proteins 59 (2005) 644–647.

[105] B.G. Guimaraes, H. Souchon, N. Honore, B. Saint-Joanis, R. Brosch, W. Shepard, S.T. Cole, P.M. Alzari, Structure and mechanism of the alkyl hydroperoxidase AhpC, a key element of the Mycobacterium tuberculosis defense system against oxidative stress, J. Biol. Chem. 280 (2005) 25735–25742.

[106] A. Kumar, A.M. Balakrishna, W. Nartey, M.S.S. Manimekalai, G. Gruber, Redox chemistry of Mycobacterium tuberculosis alkylhydroperoxide reductase E (AhpE): structural and mechanistic insight into a mycoredoxin-1 independent reductive pathway of AhpE via mycothiol, Free Radic. Biol. Med. 97 (2016) 588–601.

[107] B.S. Rho, L.W. Hung, J.M. Holton, D. Vigil, S.I. Kim, M.S. Park, T.C. Terwilliger, J. D. Pedelacq, Functional and structural characterization of a thiol peroxidase from Mycobacterium tuberculosis, J. Mol. Biol. 361 (2006) 850–863.

[108] E. Papinutto, H.J. Windle, L. Cendron, R. Battistutta, D. Kelleher, G. Zanotti, Crystal structure of alkyl hydroperoxide-reductase (AhpC) from Helicobacter pylori, Biochim. Biophys. Acta 1753 (2005) 240–246.

[109] J. Couturier, P. Prosper, A.M. Winger, A. Hecker, M. Hirasawa, D.B. Knaff, P. Gans, J.P. Jacquot, A. Navaza, A. Haouz, N. Rouhier, In the absence of thioredoxins, what are the reductants for peroxiredoxins in Thermotoga maritima? Antioxidants Redox Signal. 18 (2013) 1613–1622.

[110] I.V. Turko, L. Li, K.S. Aulak, D.J. Stuehr, J.Y. Chang, F. Murad, Protein tyrosine nitration in the mitochondria from diabetic mouse heart. Implications to dysfunctional mitochondria in diabetes, J. Biol. Chem. 278 (2003) 33972–33977.

[111] L. Randall, B. Manta, K.J. Nelson, J. Santos, L.B. Poole, A. Denicola, Structural changes upon peroxynitrite-mediated nitration of peroxiredoxin 2; nitrated Prx2

resembles its disulfide-oxidized form, Arch. Biochem. Biophys. 590 (2016) 101–108.
[112] E. Doka, T. Ida, M. Dagnell, Y. Abiko, N.C. Luong, N. Balog, T. Takata, B. Espinosa, A. Nishimura, Q. Cheng, Y. Funato, H. Miki, J.M. Fukuto, J.R. Prigge, E.E. Schmidt, E.S.J. Arner, Y. Kumagai, T. Akaike, P. Nagy, Control of protein function through oxidation and reduction of persulfidated states, Sci. Adv. 6 (2020), eaax8358.
[113] E. Cuevasanta, A.M. Reyes, A. Zeida, M. Mastrogiovanni, M.I. De Armas, R. Radi, B. Alvarez, M. Trujillo, Kinetics of formation and reactivity of the persulfide in the one-cysteine peroxiredoxin from Mycobacterium tuberculosis, J. Biol. Chem. 294 (2019) 13593–13605.
[114] J.W. Park, J.J. Mieyal, S.G. Rhee, P.B. Chock, Deglutathionylation of 2-Cys peroxiredoxin is specifically catalyzed by sulfiredoxin, J. Biol. Chem. 284 (2009) 23364–23374.
[115] A.V. Peskin, P.E. Pace, J.B. Behring, L.N. Paton, M. Soethoudt, M.M. Bachschmid, C.C. Winterbourn, Glutathionylation of the active site cysteines of peroxiredoxin 2 and recycling by glutaredoxin, J. Biol. Chem. 291 (2016) 3053–3062.
[116] D. Pastor-Flores, D. Talwar, B. Pedre, T.P. Dick, Real-time monitoring of peroxiredoxin oligomerization dynamics in living cells, Proc. Natl. Acad. Sci. U. S. A. 117 (2020) 16313–16323.
[117] H.J. Shim, S.Y. Park, H.S. Kwon, W.J. Song, T.B. Kim, K.A. Moon, J.P. Choi, S. J. Kim, Y.S. Cho, Oxidative stress modulates the expression pattern of peroxiredoxin-6 in peripheral blood mononuclear cells of asthmatic patients and bronchial epithelial cells, Allergy Asthma Immunol. Res. 12 (2020) 523–536.
[118] J. Nasu, K. Murakami, S. Miyagawa, R. Yamashita, T. Ichimura, T. Wakita, H. Hotta, T. Miyamura, T. Suzuki, T. Satoh, I. Shoji, E6AP ubiquitin ligase mediates ubiquitin-dependent degradation of peroxiredoxin 1, J. Cell. Biochem. 111 (2010) 676–685.
[119] X. Li, D. Lu, F. He, H. Zhou, Q. Liu, Y. Wang, C. Shao, Y. Gong, Cullin 4B protein ubiquitin ligase targets peroxiredoxin III for degradation, J. Biol. Chem. 286 (2011) 32344–32354.
[120] B. Chhunchha, E. Kubo, P. Singh, D.P. Singh, Sumoylation-deficient Prdx6 repairs aberrant Sumoylation-mediated Sp1 dysregulation-dependent Prdx6 repression and cell injury in aging and oxidative stress, Aging 10 (2018) 2284–2315.
[121] J. Bakovic, B.Y.K. Yu, D. Silva, S.P. Chew, S. Kim, S.H. Ahn, L. Palmer, L. Aloum, G. Stanzani, O. Malanchuk, M.R. Duchen, M. Singer, V. Filonenko, T.H. Lee, M. Skehel, I. Gout, A key metabolic integrator, coenzyme A, modulates the activity of peroxiredoxin 5 via covalent modification, Mol. Cell. Biochem. 461 (2019) 91–102.
[122] M. Hugo, K. Van Laer, A.M. Reyes, D. Vertommen, J. Messens, R. Radi, M. Trujillo, Mycothiol/mycoredoxin 1-dependent reduction of the peroxiredoxin AhpE from *Mycobacterium tuberculosis*, J. Biol. Chem. 289 (2014) 5228–5239.
[123] B. Pedre, I. Van Molle, A.F. Villadangos, K. Wahni, D. Vertommen, L. Turell, H. Erdogan, L.M. Mateos, J. Messens, The *Corynebacterium glutamicum* mycothiol peroxidase is a reactive oxygen species-scavenging enzyme that shows promiscuity in thiol redox control, Mol. Microbiol. 96 (2015) 1176–1191.
[124] B.K. Chi, T. Busche, K. Van Laer, K. Basell, D. Becher, L. Clermont, G.M. Seibold, M. Persicke, J. Kalinowski, J. Messens, H. Antelmann, Protein S-mycothiolation functions as redox-switch and thiol protection mechanism in Corynebacterium glutamicum under hypochlorite stress, Antioxidants Redox Signal. 20 (2014) 589–605.
[125] L.M. Baker, L.B. Poole, Catalytic mechanism of thiol peroxidase from Escherichia coli. Sulfenic acid formation and overoxidation of essential CYS61, J. Biol. Chem. 278 (2003) 9203–9211.
[126] W. Jeong, M.K. Cha, I.H. Kim, Thioredoxin-dependent hydroperoxide peroxidase activity of bacterioferritin comigratory protein (BCP) as a new member of the thiol-specific antioxidant protein (TSA)/Alkyl hydroperoxide peroxidase C (AhpC) family, J. Biol. Chem. 275 (2000) 2924–2930.
[127] S. Chardonnet, S. Sakr, C. Cassier-Chauvat, P. Le Marechal, F. Chauvat, S. D. Lemaire, P. Decottignies, First proteomic study of S-glutathionylation in cyanobacteria, J. Proteome Res. 14 (2015) 59–71.
[128] J.R. Harris, Release of a macromolecular protein component from human erythrocyte ghosts, Biochim. Biophys. Acta 150 (1968) 534–537.
[129] T.F. Langford, B.K. Huang, J.B. Lim, S.J. Moon, H.D. Sikes, Monitoring the action of redox-directed cancer therapeutics using a human peroxiredoxin-2-based probe, Nat. Commun. 9 (2018) 3145.
[130] M. Carmona, L. de Cubas, E. Bautista, M. Moral-Blanch, I. Medrano-Fernandez, R. Sitia, S. Boronat, J. Ayte, E. Hidalgo, Monitoring cytosolic H2O2 fluctuations arising from altered plasma membrane gradients or from mitochondrial activity, Nat. Commun. 10 (2019) 4526.
[131] B. Morgan, K. Van Laer, T.N. Owusu, D. Ezerina, D. Pastor-Flores, P.S. Amponsah, A. Tursch, T.P. Dick, Real-time monitoring of basal H2O2 levels with peroxiredoxin-based probes, Nat. Chem. Biol. 12 (2016) 437–443.
[132] V. Staudacher, M. Trujillo, T. Diederichs, T.P. Dick, R. Radi, B. Morgan, M. Deponte, Redox-sensitive GFP fusions for monitoring the catalytic mechanism and inactivation of peroxiredoxins in living cells, Redox Biol. 14 (2018) 549–556.
[133] J.R. Harris, E. Schröder, M.N. Isupov, D. Scheffler, P. Kristensen, J.A. Littlechild, A.A. Vagin, U. Meissner, Comparison of the decameric structure of peroxiredoxin-II by transmission electron microscopy and X-ray crystallography, Biochim. Biophys. Acta 1547 (2001) 221–234.
[134] M. Ardini, J.A. Huang, V. Caprettini, F. De Angelis, F. Fata, I. Silvestri, A. Cimini, F. Giansanti, F. Angelucci, R. Ippoliti, A ring-shaped protein clusters gold nanoparticles acting as molecular scaffold for plasmonic surfaces, Biochim. Biophys. Acta Gen. Subj. 1864 (2020) 129617.
[135] U. Meissner, E. Schröder, D. Scheffler, A.G. Martin, J.R. Harris, Formation, TEM study and 3D reconstruction of the human erythrocyte peroxiredoxin-2 dodecahedral higher-order assembly, Micron 38 (2007) 29–39.
[136] L.J. Domigan, H. Ashmead, S. Dimartino, J. Malmstrom, F. Grant Pearce, M. Blunt, D.E. Williams, J.A. Gerrard, Formation of supramolecular protein structures on gold surfaces, Biointerphases 12 (2017), 04E405.
[137] A.J. Phillips, J. Littlejohn, N.A. Yewdall, T. Zhu, C. Valery, F.G. Pearce, A. K. Mitra, M. Radjainia, J.A. Gerrard, Peroxiredoxin is a versatile self-assembling tecton for protein nanotechnology, Biomacromolecules 15 (2014) 1871–1881.
[138] N.A. Yewdall, T.M. Allison, F.G. Pearce, C.V. Robinson, J.A. Gerrard, Self-assembly of toroidal proteins explored using native mass spectrometry, Chem. Sci. 9 (2018) 6099–6106.
[139] T. Ando, Directly watching biomolecules in action by high-speed atomic force microscopy, Biophys. Rev. 9 (2017) 421–429.
[140] R. Charoenwattanasatien, H. Tanaka, K. Zinzius, A.K. Hochmal, R. Mutoh, D. Yamamoto, M. Hippler, G. Kurisu, X-ray crystallographic and high-speed AFM studies of peroxiredoxin 1 from Chlamydomonas reinhardtii, Acta Crystallogr. F Struct. Biol. Commun. 74 (2018) 86–91.
[141] S. Manuguri, K. Webster, N.A. Yewdall, Y. An, H. Venugopal, V. Bhugra, A. Turner, L.J. Domigan, J.A. Gerrard, D.E. Williams, J. Malmstrom, Assembly of protein stacks with in situ synthesized nanoparticle cargo, Nano Lett. 18 (2018) 5138–5145.
[142] G.K. Ahuie, H. Gagnon, P.E. Pace, A.V. Peskin, R.J. Wagner, S. Naylor, K. Klarskov, Investigating protein thiol chemistry associated with dehydroascorbate, homocysteine and glutathione using mass spectrometry, Rapid Commun. Mass Spectrom. 34 (2020), e8774.
[143] A.C. Haynes, J. Qian, J.A. Reisz, C.M. Furdui, W.T. Lowther, Molecular basis for the resistance of human mitochondrial 2-Cys peroxiredoxin 3 to hyperoxidation, J. Biol. Chem. 288 (2013) 29714–29723.
[144] I.K. Song, J.J. Lee, J.H. Cho, J. Jeong, D.H. Shin, K.J. Lee, Degradation of redox-sensitive proteins including peroxiredoxins and DJ-1 is promoted by oxidation-induced conformational changes and ubiquitination, Sci. Rep. 6 (2016) 34432.
[145] K. Kitano, Y. Niimura, Y. Nishiyama, K. Miki, Stimulation of peroxidase activity by decamerization related to ionic strength: AhpC protein from Amphibacillus xylanus, J. Biochem. 126 (1999) 313–319.
[146] C. Brachmann, L. Kaduhr, A. Judes, K.E. Ravichandran, J.D. West, S. Glatt, R. Schaffrath, Redox requirements for ubiquitin-like urmylation of Ahp1, a 2-Cys peroxiredoxin from yeast, Redox Biol. 30 (2020) 101438.
[147] M.A. Loberg, J.E. Hurtig, A.H. Graff, K.M. Allan, J.A. Buchan, M.K. Spencer, J. E. Kelly, J.E. Clodfelter, K.A. Morano, W.T. Lowther, J.D. West, Aromatic residues at the dimer-dimer interface in the peroxiredoxin Tsa1 facilitate decamer formation and biological function, Chem. Res. Toxicol. 32 (2019) 474–483.
[148] S. Shahnaj, R.K. Chowhan, P.A. Meetei, P. Kakchingtabam, K. Herojit Singh, L. Rajendrakumar Singh, P. Nongdam, A.B. Fisher, H. Rahaman, Hyperoxidation of peroxiredoxin 6 induces alteration from dimeric to oligomeric state, Antioxidants 8 (2019).
[149] J.A. Semelak, F. Battistini, R. Radi, M. Trujillo, A. Zeida, D.A. Estrin, Multiscale modeling of thiol overoxidation in peroxiredoxins by hydrogen peroxide, J. Chem. Inf. Model. 60 (2020) 843–853.
[150] S. Portillo-Ledesma, F. Sardi, B. Manta, M.V. Tourn, A. Clippe, B. Knoops, B. Alvarez, E.L. Coitino, G. Ferrer-Sueta, Deconstructing the catalytic efficiency of peroxiredoxin-5 peroxidatic cysteine, Biochemistry 53 (2014) 6113–6125.
[151] B.B. Horta, M.A. de Oliveira, K.F. Discola, J.R. Cussiol, L.E. Netto, Structural and biochemical characterization of peroxiredoxin Qbeta from Xylella fastidiosa: catalytic mechanism and high reactivity, J. Biol. Chem. 285 (2010) 16051–16065.
[152] A. Echalier, X. Trivelli, C. Corbier, N. Rouhier, O. Walker, P. Tsan, J.P. Jacquot, A. Aubry, I. Krimm, J.M. Lancelin, Crystal structure and solution NMR dynamics of a D (type II) peroxiredoxin glutaredoxin and thioredoxin dependent: a new insight into the peroxiredoxin oligomerism, Biochemistry 44 (2005) 1755–1767.
[153] S. Barelier, D. Linard, J. Pons, A. Clippe, B. Knoops, J.M. Lancelin, I. Krimm, Discovery of fragment molecules that bind the human peroxiredoxin 5 active site, PLoS One 5 (2010), e9744.
[154] J. Aden, M. Wallgren, P. Storm, C.F. Weise, A. Christiansen, W.P. Schröder, C. Funk, M. Wolf-Watz, Extraordinary mus-ms backbone dynamics in Arabidopsis thaliana peroxiredoxin Q, Biochim. Biophys. Acta 1814 (2011) 1880–1890.
[155] G.W. Buchko, A. Perkins, D. Parsonage, L.B. Poole, P.A. Karplus, Backbone chemical shift assignments for Xanthomonas campestris peroxiredoxin Q in the reduced and oxidized states: a dramatic change in backbone dynamics, Biomol. NMR Assign 10 (2016) 57–61.
[156] D.Y. Lee, S.J. Park, W. Jeong, H.J. Sung, T. Oho, X. Wu, S.G. Rhee, J.M. Gruschus, Mutagenesis and modeling of the peroxiredoxin (Prx) complex with the NMR structure of ATP-bound human sulfiredoxin implicate aspartate 187 of Prx I as the catalytic residue in ATP hydrolysis, Biochemistry 45 (2006) 15301–15309.
[157] C. Raingeval, O. Cala, B. Brion, M. Le Borgne, R.E. Hubbard, I. Krimm, 1D NMR WaterLOGSY as an efficient method for fragment-based lead discovery, J. Enzym. Inhib. Med. Chem. 34 (2019) 1218–1225.
[158] X. Trivelli, I. Krimm, C. Ebel, L. Verdoucq, V. Prouzet-Mauleon, Y. Chartier, P. Tsan, G. Lauquin, Y. Meyer, J.M. Lancelin, Characterization of the yeast peroxiredoxin Ahp1 in its reduced active and overoxidized inactive forms using NMR, Biochemistry 42 (2003) 14139–14149.
[159] M. Khoshouei, M. Radjainia, A.J. Phillips, J.A. Gerrard, A.K. Mitra, J.M. Plitzko, W. Baumeister, R. Danev, Volta phase plate cryo-EM of the small protein complex Prx3, Nat. Commun. 7 (2016) 10534.
[160] M. Radjainia, H. Venugopal, A. Desfosses, A.J. Phillips, N.A. Yewdall, M. B. Hampton, J.A. Gerrard, A.K. Mitra, Cryo-electron microscopy structure of

human peroxiredoxin-3 filament reveals the assembly of a putative chaperone, Structure 23 (2015) 912–920.
[161] S. Rinalducci, G.M. D'Amici, B. Blasi, L. Zolla, Oxidative stress-dependent oligomeric status of erythrocyte peroxiredoxin II (PrxII) during storage under standard blood banking conditions, Biochimie 93 (2011) 845–853.
[162] Y. Yan, P. Sabharwal, M. Rao, S. Sockanathan, The antioxidant enzyme Prdx1 controls neuronal differentiation by thiol-redox-dependent activation of GDE2, Cell 138 (2009) 1209–1221.
[163] M. Gertz, F. Fischer, M. Leipelt, D. Wolters, C. Steegborn, Identification of Peroxiredoxin 1 as a novel interaction partner for the lifespan regulator protein p66Shc, Aging 1 (2009) 254–265.
[164] H. Nassour, Z. Wang, A. Saad, A. Papaluca, N. Brosseau, B. Affar el, M.A. Alaoui-Jamali, D. Ramotar, Peroxiredoxin 1 interacts with and blocks the redox factor APE1 from activating interleukin-8 expression, Sci. Rep. 6 (2016) 29389.
[165] L. Deng, X. Gan, M. Ito, M. Chen, H.H. Aly, C. Matsui, T. Abe, K. Watashi, T. Wakita, T. Suzuki, T. Okamoto, Y. Matsuura, M. Mizokami, I. Shoji, H. Hotta, Peroxiredoxin 1, a novel HBx-interacting protein, interacts with exosome component 5 and negatively regulates hepatitis B virus (HBV) propagation through degradation of HBV RNA, J. Virol. 93 (2019).
[166] A. Matte, M. Bertoldi, N. Mohandas, X. An, A. Bugatti, A.M. Brunati, M. Rusnati, E. Tibaldi, A. Siciliano, F. Turrini, S. Perrotta, L. De Franceschi, Membrane association of peroxiredoxin-2 in red cells is mediated by the N-terminal cytoplasmic domain of band 3, Free Radic. Biol. Med. 55 (2013) 27–35.
[167] P.E. Pace, A.V. Peskin, M.H. Han, M.B. Hampton, C.C. Winterbourn, Hyperoxidized peroxiredoxin 2 interacts with the protein disulfide- isomerase ERp46, Biochem. J. 453 (2013) 475–485.
[168] R.B. Moore, M.V. Mankad, S.K. Shriver, V.N. Mankad, G.A. Plishker, Reconstitution of Ca(2+)-dependent K+ transport in erythrocyte membrane vesicles requires a cytoplasmic protein, J. Biol. Chem. 266 (1991) 18964–18968.
[169] D.H. Kang, D.J. Lee, K.W. Lee, Y.S. Park, J.Y. Lee, S.H. Lee, Y.J. Koh, G.Y. Koh, C. Choi, D.Y. Yu, J. Kim, S.W. Kang, Peroxiredoxin II is an essential antioxidant enzyme that prevents the oxidative inactivation of VEGF receptor-2 in vascular endothelial cells, Mol. Cell. 44 (2011) 545–558.
[170] N. Xiao, G. Du, M.A. Frohman, Peroxiredoxin II functions as a signal terminator for H2O2-activated phospholipase D1, FEBS J. 272 (2005) 3929–3937.
[171] R.H. Malty, H. Aoki, A. Kumar, S. Phanse, S. Amin, Q. Zhang, Z. Minic, F. Goebels, G. Musso, Z. Wu, H. Abou-Tok, M. Meyer, V. Deineko, S. Kassir, V. Sidhu, M. Jessulat, N.E. Scott, X. Xiong, J. Vlasblom, B. Prasad, L.J. Foster, T. Alberio, B. Garavaglia, H. Yu, G.D. Bader, K. Nakamura, J. Parkinson, M. Babu, A map of human mitochondrial protein interactions linked to neurodegeneration reveals new mechanisms of redox homeostasis and NF-kappaB signaling, Cell Syst. 5 (2017) 564–577, e512.
[172] S.S. Schattauer, B.B. Land, K.L. Reichard, A.D. Abraham, L.M. Burgeno, J. R. Kuhar, P.E.M. Phillips, S.E. Ong, C. Chavkin, Peroxiredoxin 6 mediates Galphai protein-coupled receptor inactivation by cJun kinase, Nat. Commun. 8 (2017) 743.
[173] G.Y. Liu, J.X. Shi, S.L. Shi, F. Liu, G. Rui, X. Li, L.B. Gao, X.L. Deng, Q.F. Li, Nucleophosmin regulates intracellular oxidative stress homeostasis via antioxidant PRDX6, J. Cell. Biochem. 118 (2017) 4697–4707.
[174] C. Dasari, K.R.K. Reddy, S. Natani, T.R.L. Murthy, S. Bhukya, R. Ummanni, Tumor protein D52 (isoform 3) interacts with and promotes peroxidase activity of Peroxiredoxin 1 in prostate cancer cells implicated in cell growth and migration, Biochim. Biophys. Acta Mol. Cell Res. 1866 (2019) 1298–1309.
[175] C. Vascotto, D. Fantini, M. Romanello, L. Cesaratto, M. Deganuto, A. Leonardi, J. P. Radicella, M.R. Kelley, C. D'Ambrosio, A. Scaloni, F. Quadrifoglio, G. Tell, APE1/Ref-1 interacts with NPM1 within nucleoli and plays a role in the rRNA quality control process, Mol. Cell Biol. 29 (2009) 1834–1854.
[176] U. Schwertassek, Y. Balmer, M. Gutscher, L. Weingarten, M. Preuss, J. Engelhard, M. Winkler, T.P. Dick, Selective redox regulation of cytokine receptor signaling by extracellular thioredoxin-1, EMBO J. 26 (2007) 3086–3097.
[177] R. Chang, E. Wang, Mouse translation elongation factor eEF1A-2 interacts with Prdx-I to protect cells against apoptotic death induced by oxidative stress, J. Cell. Biochem. 100 (2007) 267–278.
[178] S.T. Wen, R.A. Van Etten, The PAG gene product, a stress-induced protein with antioxidant properties, is an Abl SH3-binding protein and a physiological inhibitor of c-Abl tyrosine kinase activity, Genes Dev. 11 (1997) 2456–2467.
[179] Z.M. Mu, X.Y. Yin, E.V. Prochownik, Pag, a putative tumor suppressor, interacts with the Myc Box II domain of c-Myc and selectively alters its biological function and target gene expression, J. Biol. Chem. 277 (2002) 43175–43184.
[180] H. Jung, T. Kim, H.Z. Chae, K.T. Kim, H. Ha, Regulation of macrophage migration inhibitory factor and thiol-specific antioxidant protein PAG by direct interaction, J. Biol. Chem. 276 (2001) 15504–15510.
[181] S.K. Hong, M.K. Cha, I.H. Kim, Specific protein interaction of human Pag with Omi/HtrA2 and the activation of the protease activity of Omi/HtrA2, Free Radic. Biol. Med. 40 (2006) 275–284.
[182] D.C. Angeles, B.H. Gan, L. Onstead, Y. Zhao, K.L. Lim, J. Dachsel, H. Melrose, M. Farrer, Z.K. Wszolek, D.W. Dickson, E.K. Tan, Mutations in LRRK2 increase phosphorylation of peroxiredoxin 3 exacerbating oxidative stress-induced neuronal death, Hum. Mutat. 32 (2011) 1390–1397.
[183] Y. Feng, D.Q. Liu, Z. Wang, Z. Liu, H.Q. Cao, L.Y. Wang, N. Shi, X.M. Meng, AOP-1 interacts with cardiac-specific protein kinase TNNI3K and down-regulates its kinase activity, Biochemistry (Mosc.) 72 (2007) 1199–1204.
[184] M. Masaki, A. Ikeda, E. Shiraki, S. Oka, T. Kawasaki, Mixed lineage kinase LZK and antioxidant protein-1 activate NF-kappaB synergistically, Eur. J. Biochem. 270 (2003) 76–83.
[185] G. Vaz Meirelles, D.C. Ferreira Lanza, J.C. da Silva, J. Santana Bernachi, A.F. Paes Leme, J. Kobarg, Characterization of hNek6 interactome reveals an important role for its short N-terminal domain and colocalization with proteins at the centrosome, J. Proteome Res. 9 (2010) 6298–6316.
[186] L. Liu, C. Yang, J. Yuan, X. Chen, J. Xu, Y. Wei, J. Yang, G. Lin, L. Yu, RPK118, a PX domain-containing protein, interacts with peroxiredoxin-3 through pseudo-kinase domains, Mol Cells 19 (2005) 39–45.
[187] D.Y. Jin, H.Z. Chae, S.G. Rhee, K.T. Jeang, Regulatory role for a novel human thioredoxin peroxidase in NF-kappaB activation, J. Biol. Chem. 272 (1997) 30952–30961.
[188] P. Giguere, M.E. Turcotte, E. Hamelin, A. Parent, J. Brisson, G. Laroche, P. Labrecque, G. Dupuis, J.L. Parent, Peroxiredoxin-4 interacts with and regulates the thromboxane A(2) receptor, FEBS Lett. 581 (2007) 3863–3868.
[189] S.L. Sorrell, Z.J. Golder, D.B. Johnstone, F.E.K. Frankl, Renal peroxiredoxin 6 interacts with anion exchanger 1 and plays a novel role in pH homeostasis, Kidney Int. 89 (2016) 105–112.
[190] J. Kwon, A. Wang, D.J. Burke, H.E. Boudreau, K.J. Lekstrom, A. Korzeniowska, R. Sugamata, Y.S. Kim, L. Yi, I. Ersoy, S. Jaeger, K. Palaniappan, D.R. Ambruso, S. H. Jackson, T.L. Leto, Peroxiredoxin 6 (Prdx6) supports NADPH oxidase1 (Nox1)-based superoxide generation and cell migration, Free Radic. Biol. Med. 96 (2016) 99–115.
[191] R.B. Moore, S.K. Shriver, Protein 7.2b of human erythrocyte membranes binds to calpromotin, Biochem. Biophys. Res. Commun. 232 (1997) 294–297.
[192] S. Zhou, Y.C. Lien, T. Shuvaeva, K. DeBolt, S.I. Feinstein, A.B. Fisher, Functional interaction of glutathione S-transferase pi and peroxiredoxin 6 in intact cells, Int. J. Biochem. Cell Biol. 45 (2013) 401–407.
[193] M.H. Choi, I.K. Lee, G.W. Kim, B.U. Kim, Y.H. Han, D.Y. Yu, H.S. Park, K.Y. Kim, J.S. Lee, C. Choi, Y.S. Bae, B.I. Lee, S.G. Rhee, S.W. Kang, Regulation of PDGF signalling and vascular remodelling by peroxiredoxin II, Nature 435 (2005) 347–353.
[194] S.Y. Park, X. Yu, C. Ip, J.L. Mohler, P.N. Bogner, Y.M. Park, Peroxiredoxin 1 interacts with androgen receptor and enhances its transactivation, Canc. Res. 67 (2007) 9294–9303.
[195] J.R. Riddell, X.Y. Wang, H. Minderman, S.O. Gollnick, Peroxiredoxin 1 stimulates secretion of proinflammatory cytokines by binding to TLR4, J. Immunol. 184 (2010) 1022–1030.
[196] Y.J. Kim, W.S. Lee, C. Ip, H.Z. Chae, E.M. Park, Y.M. Park, Prx1 suppresses radiation-induced c-Jun NH2-terminal kinase signaling in lung cancer cells through interaction with the glutathione S-transferase Pi/c-Jun NH2-terminal kinase complex, Canc. Res. 66 (2006) 7136–7142.
[197] J. Cao, J. Schulte, A. Knight, N.R. Leslie, A. Zagozdzon, R. Bronson, Y. Manevich, C. Beeson, C.A. Neumann, Prdx1 inhibits tumorigenesis via regulating PTEN/AKT activity, EMBO J. 28 (2009) 1505–1517.
[198] B.L. Hopkins, M. Nadler, J.J. Skoko, T. Bertomeu, A. Pelosi, P.M. Shafaei, K. Levine, A. Schempf, B. Pennarun, B. Yang, D. Datta, O. Bucur, K. Ndebele, S. Oesterreich, D. Yang, M. Giulia Rizzo, R. Khosravi-Far, C.A. Neumann, A peroxidase peroxiredoxin 1-specific redox regulation of the novel FOXO3 microRNA target let-7, Antioxidants Redox Signal. 28 (2018) 62–77.
[199] V. Tosello, V. Saccomani, J. Yu, F. Bordin, A. Amadori, E. Piovan, Calcineurin complex isolated from T-cell acute lymphoblastic leukemia (T-ALL) cells identifies new signaling pathways including mTOR/AKT/S6K whose inhibition synergize with calcineurin inhibition to promote T-ALL cell death, Oncotarget 7 (2016) 45715–45729.
[200] Y. Min, M.J. Kim, S. Lee, E. Chun, K.Y. Lee, Inhibition of TRAF6 ubiquitin-ligase activity by PRDX1 leads to inhibition of NFKB activation and autophagy activation, Autophagy 14 (2018) 1347–1358.
[201] X. Wang, S. He, J.M. Sun, G.P. Delcuve, J.R. Davie, Selective association of peroxiredoxin 1 with genomic DNA and COX-2 upstream promoter elements in estrogen receptor negative breast cancer cells, Mol. Biol. Cell 21 (2010) 2987–2995.
[202] D.H. Kang, D.J. Lee, S. Lee, S.Y. Lee, Y. Jun, Y. Kim, Y. Kim, J.S. Lee, D.K. Lee, S. Lee, E.H. Jho, D.Y. Yu, S.W. Kang, Interaction of tankyrase and peroxiredoxin II is indispensable for the survival of colorectal cancer cells, Nat. Commun. 8 (2017) 40.
[203] X. Chen, X. Cao, W. Xiao, B. Li, Q. Xue, PRDX5 as a novel binding partner in Nrf2-mediated NSCLC progression under oxidative stress, Aging 12 (2020) 122–137.
[204] B. Chhunchha, E. Kubo, N. Fatma, D.P. Singh, Sumoylation-deficient Prdx6 gains protective function by amplifying enzymatic activity and stability and escapes oxidative stress-induced aberrant Sumoylation, Cell Death Dis. 8 (2017) e2525.
[205] S. Lipinski, S. Pfeuffer, P. Arnold, C. Treitz, K. Aden, H. Ebsen, M. Falk-Paulsen, N. Gisch, A. Fazio, J. Kuiper, A. Luzius, S. Billmann-Born, S. Schreiber, G. Nunez, H.D. Beer, T. Strowig, M. Lamkanfi, A. Tholey, P. Rosenstiel, Prdx4 limits caspase-1 activation and restricts inflammasome-mediated signaling by extracellular vesicles, EMBO J. 38 (2019), e101266.
[206] T.J. Tavender, J.J. Springate, N.J. Bulleid, Recycling of peroxiredoxin IV provides a novel pathway for disulphide formation in the endoplasmic reticulum, EMBO J. 29 (2010) 4185–4197.
[207] H. Horita, A. Law, S. Hong, K. Middleton, A simple toolset to identify endogenous post-translational modifications for a target protein: a snapshot of the EGFR signaling pathway, Biosci. Rep. 37 (2017).
[208] D.M. Svistunova, J.N. Simon, E. Rembeza, M. Crabtree, W.W. Yue, P.L. Oliver, M. J. Finelli, Oxidation resistance 1 regulates post-translational modifications of peroxiredoxin 2 in the cerebellum, Free Radic. Biol. Med. 130 (2019) 151–162.
[209] L.M. Randall, B. Manta, M. Hugo, M. Gil, C. Batthyany, M. Trujillo, L.B. Poole, A. Denicola, Nitration transforms a sensitive peroxiredoxin 2 into a more active and robust peroxidase, J. Biol. Chem. 289 (2014) 15536–15543.

[210] T.T. Reed, W.M. Pierce Jr., D.M. Turner, W.R. Markesbery, D.A. Butterfield, Proteomic identification of nitrated brain proteins in early Alzheimer's disease inferior parietal lobule, J. Cell Mol. Med. 13 (2009) 2019–2029.
[211] Z. Sun, B.P. Chadwick, Loss of SETDB1 decompacts the inactive X chromosome in part through reactivation of an enhancer in the IL1RAPL1 gene, Epigenet. Chromatin 11 (2018) 45.
[212] C.S. Gibhardt, S. Cappello, R. Bhardwaj, R. Schober, S.A. Kirsch, Z. Bonilla Del Rio, S. Gahbauer, A. Bochicchio, M. Sumanska, C. Ickes, I. Stejerean-Todoran, M. Mitkovski, D. Alansary, X. Zhang, A. Revazian, M. Fahrner, V. Lunz, I. Frischauf, T. Luo, D. Ezerina, J. Messens, V.V. Belousov, M. Hoth, R. A. Bockmann, M.A. Hediger, R. Schindl, I. Bogeski, Oxidative stress-induced STIM2 cysteine modifications suppress store-operated calcium entry, Cell Rep. 33 (2020) 108292.
[213] B.K. Chi, A.A. Roberts, T.T. Huyen, K. Basell, D. Becher, D. Albrecht, C. J. Hamilton, H. Antelmann, S-bacillithiolation protects conserved and essential proteins against hypochlorite stress in firmicutes bacteria, Antioxidants Redox Signal. 18 (2013) 1273–1295.
[214] M. Hillion, J. Bernhardt, T. Busche, M. Rossius, S. Maass, D. Becher, M. Rawat, M. Wirtz, R. Hell, C. Ruckert, J. Kalinowski, H. Antelmann, Monitoring global protein thiol-oxidation and protein S-mycothiolation in Mycobacterium smegmatis under hypochlorite stress, Sci. Rep. 7 (2017) 1195.
[215] M. Hillion, M. Imber, B. Pedre, J. Bernhardt, M. Saleh, V.V. Loi, S. Maass, D. Becher, L. Astolfi Rosado, L. Adrian, C. Weise, R. Hell, M. Wirtz, J. Messens, H. Antelmann, The glyceraldehyde-3-phosphate dehydrogenase GapDH of *Corynebacterium diphtheriae* is redox-controlled by protein S-mycothiolation under oxidative stress, Sci. Rep. 7 (2017) 5020.
[216] Y. Tsuchiya, A. Zhyvoloup, J. Bakovic, N. Thomas, B.Y.K. Yu, S. Das, C. Orengo, C. Newell, J. Ward, G. Saladino, F. Comitani, F.L. Gervasio, O.M. Malanchuk, A. I. Khoruzhenko, V. Filonenko, S.Y. Peak-Chew, M. Skehel, I. Gout, Protein CoAlation and antioxidant function of coenzyme A in prokaryotic cells, Biochem. J. 475 (2018) 1909–1937.
[217] M.H. Lin, T.L. Hsu, S.Y. Lin, Y.J. Pan, J.T. Jan, J.T. Wang, K.H. Khoo, S.H. Wu, Phosphoproteomics of Klebsiella pneumoniae NTUH-K2044 reveals a tight link between tyrosine phosphorylation and virulence, Mol. Cell. Proteomics 8 (2009) 2613–2623.
[218] J. Zhang, R. Sprung, J. Pei, X. Tan, S. Kim, H. Zhu, C.F. Liu, N.V. Grishin, Y. Zhao, Lysine acetylation is a highly abundant and evolutionarily conserved modification in Escherichia coli, Mol. Cell. Proteomics 8 (2009) 215–225.
[219] B. Macek, F. Gnad, B. Soufi, C. Kumar, J.V. Olsen, I. Mijakovic, M. Mann, Phosphoproteome analysis of E. coli reveals evolutionary conservation of bacterial Ser/Thr/Tyr phosphorylation, Mol. Cell. Proteomics 7 (2008) 299–307.
[220] M.H. Lin, N. Sugiyama, Y. Ishihama, Systematic profiling of the bacterial phosphoproteome reveals bacterium-specific features of phosphorylation, Sci. Signal. 8 (2015) rs10.
[221] N.C. Soares, P. Spat, K. Krug, B. Macek, Global dynamics of the Escherichia coli proteome and phosphoproteome during growth in minimal medium, J. Proteome Res. 12 (2013) 2611–2621.
[222] P. Spat, B. Macek, K. Forchhammer, Phosphoproteome of the cyanobacterium Synechocystis sp. PCC 6803 and its dynamics during nitrogen starvation, Front. Microbiol. 6 (2015) 248.
[223] M. Angeleri, D. Muth-Pawlak, E.M. Aro, N. Battchikova, Study of O-phosphorylation sites in proteins involved in photosynthesis-related processes in synechocystis sp. strain PCC 6803: application of the SRM approach, J. Proteome Res. 15 (2016) 4638–4652.
[224] C.L. Lawson, A. Patwardhan, M.L. Baker, C. Hryc, E.S. Garcia, B.P. Hudson, I. Lagerstedt, S.J. Ludtke, G. Pintilie, R. Sala, J.D. Westbrook, H.M. Berman, G. J. Kleywegt, W. Chiu, EMDataBank unified data resource for 3DEM, Nucleic Acids Res. 44 (2016) D396–D403.
[225] D. Shi, B.L. Nannenga, M.G. Iadanza, T. Gonen, Three-dimensional electron crystallography of protein microcrystals, Elife 2 (2013), e01345.
[226] M.P. Blakeley, S.S. Hasnain, S.V. Antonyuk, Sub-atomic resolution X-ray crystallography and neutron crystallography: promise, challenges and potential, IUCrJ 2 (2015) 464–474.
[227] Y. Yan, H. Tao, J. He, S.Y. Huang, The HDOCK server for integrated protein-protein docking, Nat. Protoc. 15 (2020) 1829–1852.
[228] H.N. Chua, K. Ning, W.K. Sung, H.W. Leong, L. Wong, Using indirect protein-protein interactions for protein complex prediction, J. Bioinf. Comput. Biol. 6 (2008) 435–466.
[229] M. Kohler, C. Neff, C. Perez, C. Brunner, E. Pardon, J. Steyaert, G. Schneider, K. P. Locher, R. Zenobi, Binding specificities of Nanobody*Membrane protein complexes obtained from chemical cross-linking and high-mass MALDI mass spectrometry, Anal. Chem. 90 (2018) 5306–5313.
[230] G. Young, N. Hundt, D. Cole, A. Fineberg, J. Andrecka, A. Tyler, A. Olerinyova, A. Ansari, E.G. Marklund, M.P. Collier, S.A. Chandler, O. Tkachenko, J. Allen, M. Crispin, N. Billington, Y. Takagi, J.R. Sellers, C. Eichmann, P. Selenko, L. Frey, R. Riek, M.R. Galpin, W.B. Struwe, J.L.P. Benesch, P. Kukura, Quantitative mass imaging of single biological macromolecules, Science 360 (2018) 423–427.
[231] D. Clift, W.A. McEwan, L.I. Labzin, V. Konieczny, B. Mogessie, L.C. James, M. Schuh, A method for the acute and rapid degradation of endogenous proteins, Cell 171 (2017) 1692–1706, e1618.
[232] S. Pfeffer, J. Mahamid, Unravelling molecular complexity in structural cell biology, Curr. Opin. Struct. Biol. 52 (2018) 111–118.